Carbonates and Evaporites (2023) 38:2
https://doi.org/10.1007/s13146-022-00818-w

REVIEW ARTICLE

Environmental characteristics and unified failure mode classification system for mining landslides in the karst mountainous areas of southwestern China

Zuliang Zhong[1,2,3] · Yawei Xu[1] · Nanyun Wang[1] · Xinrong Liu[1,2,3] · Guofu Gao[1]

Accepted: 17 July 2022 / Published online: 12 November 2022

Abstract

The karst mountainous areas of southwestern China are widely distributed and affluent in mineral resources. However, mining activities induced numerous large-scale landslides in this area, resulting in tremendous loss of lives and property to residents. As a result, it is crucial to figure out the triggering mechanism and failure modes of mining landslides for landslide prevention. In this paper, the environment characteristics and triggering mechanism of mining landslides in karst mountainous areas of southwestern China were analyzed by investigating a few mining landslides. Specifically, it can be attributed to the natural environment and human activities, which are topography, lithology, geological structure, karst hydrogeology, rainfall, and mining activities. On the other hand, a unified failure mode classification system for mining landslides in karst mountainous areas of Southwest China was established based on the international landslide classification system and different slope structures (subhorizontal bedding layered slope, bedding layered slope, anti-dip layered slope, lateral layered slope, oblique inclined bedding layered slope). In this classification system, the basic failure modes were analyzed in detail, and the mining impact mechanisms for each failure mode were revealed. The corresponding mechanical models and stability criteria for mining-induced flexural topple and planar slide were summarized. This study not only identifies and rapidly classifies mining landslides in the karst mountainous areas of southwestern China, but also further facilitates the prediction and evaluation of the stability of mining-induced unstable rock masses.

Keywords Karst mountainous areas in southwestern China · Mining landslides · Environmental characteristics · Failure mode classification system · Different slope types · Mechanical model

Introduction

Mining landslide, directly resulting from or related to mining activities, is usually accompanied by high-speed and long run-out debris flow or other destructive disasters (Yu and Mao 2020), causing numerous disasters all over the world, such as the Frank slide (Benko and Stead 1998), Aberfan landslide (Bentley and Siddle 1996), Nattai North landslide (Salmi et al. 2017; Do and Wu 2020), Ostrava–Karviná landslide (Marian et al. 2012a, b), Yanchihe landslide (Chen et al. 2018), and Jiweishan landslide (Ge et al. 2019). Due to fast movement, complex geological environment, uncertain failure mechanism and difficult identification, mining landslides threaten the lives of people and the safety of major projects in mountainous areas. Therefore, the study on large-scale mining landslides is of critical importance in the research of international landslides.

In recent years, the formative factors and environmental characteristics of mining landslide have been studied. Tang (2009) summarized the formation conditions of mining landslide into three essential factors: underground mining, sloping ground and weak interlayer, while mining activities can destroy the hydrological and geologic environment of the upper strata. Erginal et al. (2008) attempted to reveal the

✉ Zuliang Zhong
haiou983@126.com

1 College of Civil Engineering, Chongqing University, Chongqing 400045, China

2 National Joint Engineering Research Center for Prevention and Control of Environmental Geological Hazards in the TGR Area Chongqing University, Chongqing 400045, China

3 State Key Laboratory of Coal Mine Disaster Dynamics and Control, Chongqing University, Chongqing 400045, China

influence of mining which induced deep-seated landslide in the Bursa Orhaneli lignite field of northwestern Turkey, and proposed that the dynamic response generated by mining would aggravate the damage of the slope. Moreover, Nunoo (2018) indicated that the occurrence of slope instability resulted from variation of mining equipment, impact of mining blasting and some natural factors. Zhang et al. (2016) studied the mining depth–thickness ratio to figure out the stability of the mining slope and determined that the depth of mining activities greatly influenced the deformation. For better understanding of the formation mechanism of mining landslides, field investigation, site monitoring and numerical simulation methods were used to analyze the unstable rock masses in Wulong area of Chongqing, China. Li et al. (2017) proposed that the dominant crack also plays a significant role in forming landslides in mining areas. Arca et al. (2018) investigated the mining-induced landslides in Kozlu, Turkey, and the results showed that mining landslides were more common in karst areas because of the easy dissolution of carbonate rocks.

As the center of karst mountainous areas in Southwest China, Guizhou with other surrounding provinces forms one of the three global karst areas, which covers over 5.1×10^5 km^2 and has intense karst phenomenon (Li et al. 2019; Wang et al. 2020). It is also located in the convergence zone of the Eurasian, Indian, and Pacific plate, which has good mineralization geological conditions (Fig. 1). More than 155 kinds of minerals and 11,000 mineral deposits have been discovered, proving it to be one of the best mineral resource development areas in China (Jian et al. 2014; Zhu et al. 2019). Unfortunately, frequent mineral exploitation not only destroys karst ecological environment, but also results in a series of large-scale geological disasters, among which the mining landslides is the most catastrophic (Zhu et al. 2019; Lv et al. 2018) (Table 1). Beyond that, there are a huge number of mining-induced unstable rock masses: Zengziyan Cliff has 73 blocks of unstable rock masses (He et al. 2019a), Wangxia Cliff has more than 1.2 million m^3 of unstable rock masses (Wang and Li 2009), and Lianziya Cliff has 2.16 million m^3 of unstable rock masses (He et al. 2009). Due to slow deformation, these unstable rock masses will undoubtedly produce catastrophic disasters in the future.

Considerable studies on failure modes and formation mechanisms for mining-induced landslide in karst mountainous areas of southwestern China have been conducted. It is believed that geological structure, karst, and underground mining were of primary importance in triggering the Jiweishan landslide (Feng et al. 2016). Xu et al. (2014) proposed that the crushing of the key rock mass by mining excavation resulted in a subsequent apparent dip slide. Zheng et al. (2015) investigated 46 unstable rock masses in Kaiyang area, and the failure modes in this area were controlled by structural characteristics such as crack toppling, crack sliding and crack slumping. Lin et al. (2018) carried out field investigation, deformation monitoring and numerical analysis on Xiaoba landslide in Fuquan, in which a geomechanical mode of sliding tension–shear for bedding layered slopes is proposed. Li et al. (2016a) divided the failure process of Jiguanling landslide into four stages: long-term bending,

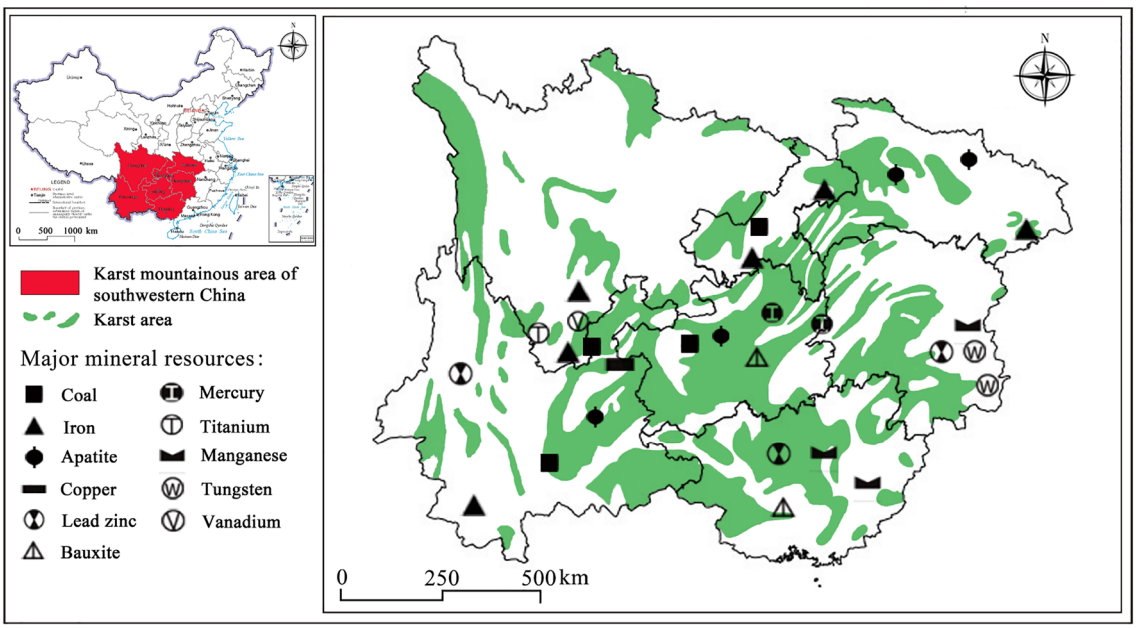

Fig. 1 Distribution of the karst and mineral resources in the mountainous area of southwestern China

Table 1 Mining landslides and its hazard in the karst mountainous areas of southwestern China

Mining landslides	Time	Location	Minerals	Hazard
The Yanchihe landslide	1980	Yichang, Hubei	Phosphorite	284 people died, a large number of buildings were destroyed
The Kaiyang landslide	1980	Kaiyang, Guizhou	Phosphorite	Blocked the Yangshui River, formed a barrier lake
The Zhongyangcun landslide	1988	Wuxi, Chongqing	Coal	26 people died, 7 people were injured, economic loss was 4.685 million yuan
The Jiguanling landslide	1994	Wulong, Chongqing	Coal	17 people died, 19 people were injured, economic loss was 100 million yuan
The Laojinshan landslide	1996	Yuanyang, Yunnan	Gold	111 people died, 116 missing, 16 seriously injured
The Zuojiaying landslide	2004	Nayong, Guizhou	Coal	44 people died
The Zengziyan W12 landslide	2004	Nanchuan, Chongqing	Bauxite	Threatened the lives of 564 people
The Madaling landslide	2006	Duyun, Guizhou	Coal	Flooded a lot of farmland
The Yaoyanjiao landslide	2006	Houchang, Guizhou	Coal	Large-scale unstable rock masses remained
The Jiweishan landslide	2009	Wulong, Chongqing	Iron	74 people died, 8 people were injured, 12 houses were buried
The Wangxia W2-2 landslide	2010	Wushan, Chongqing	Coal	Threatened the lives of 400 people
The Honglianchi landslide	2012	Hefeng, Hubei	Iron	Threatened the lives of 13 people
The Yudong landslide	2013	Kaili, Guizhou	Coal	5 people died, 6 houses were buried
The Xiaoba landslide	2014	Fuquan, Guizhou	Phosphorite	23 people died, 22 people were injured, 77 houses were buried
The Pusa landslide	2017	Nayong, Guizhou	Coal	35 people died, 8 people were injured

mining-induced toppling, resisting block sliding and the catastrophic rockslide.

Though the above studies introduced some typical cases in karst mountainous areas of southwestern China, none of them systematically unified the mining-induced landslide failure modes classification system. In fact, current failure modes may result in a complicated classification of mining landslides, and it would be impossible to identify and classify a new mining landslide rapidly, which will hamper a rescue operation. In this review, the environment characteristics of large-scale mining landslides in karst mountainous areas of southwestern China were presented via investigating a few mining landslides. A unified failure mode classification system for mining landslides in karst mountainous areas of Southwest China was established, the basic failure modes were analyzed in detail, and the mining impact mechanisms for each failure mode were revealed. Also, the corresponding mechanical models and stability criteria for mining-induced flexural topple and planar slide were summarized.

Analysis of environmental characteristics

The environment characteristics for a few typical mining landslides in the karst mountainous areas of southwestern China are summarized in Table 2. It can be seen that the environmental characteristics are different from those of ordinary landslides. It is not only affected by natural factors such as topography, lithology, geological structure, karst hydrogeology and rainfall, but also closely related to man-made mining activities, the schematic diagram of which is shown in Fig. 2.

Topography

The karst mountainous area in southwestern China is in the transition zone between the second and third steps, with an average elevation of 1000–2000 m. The terrain is generally higher in the west and lower in the east. Affected by the neotectonics, the intermittently uplifted strata and strongly downward cutting of rivers result in high slopes and deep valleys. The upper part of the slope presents a steep shaped under the influence of the geological structure and self-weight, while the lower part forms a typical boot-shaped landform due to the foundation supporting force (He and Chen 2014). The boot-shaped landform and the elevation difference of over 100 m provide favorable free-face conditions for landslides.

Lithology

The southwest karst mountainous area located in the Yangtze block, which has gone through a series of continental, marine, and marine–continental depositions since the Proterozoic. The neritic carbonate stratum dominated by limestone and dolomite and the clastic stratum dominated by sandstone form dozens of meters thick hard stratum, which has excellent physical properties and high mechanical strength. However, in the areas where large-scale mining landslides occur, there are often shale, mudstone or coal-bearing soft clay strata with low mechanical parameters and

Table 2 Environmental characteristics of typical mining landslides in the karst mountainous areas of southwestern China

Landslides	Topography	Main lithology (from top to bottom)	Geological structure	Karst hydrogeology and rainfall	Mining activities
The Yaoyanjiao landslide	Plateau platform and middle elevation karst mountainous valley landform	Jiusi Formation of lower Carboniferous (C_1j): limestone with mud shale at the bottom; Xiangbai Formation of lower Carboniferous (C_1x): quartz sandstone intercalated with sandy shale, carbonaceous shale and coal seams	The strata occurrence is 270°∠4°–12°, two groups of dominant discontinuities are: J1: 32°∠86°, controls extension direction of karst gully in limestone; J2: 122°∠70°	Karst features such as karst ditches and grooves are well developed. A longitudinal corrosion discontinuity develops on the back edge of the cliff. There is a karst cave with a width of more than 20 m and a maximum depth of 3–4 m at the bottom. The annual average precipitation is 950.9 mm, and the maximum annual precipitation is 1436.5 mm, The precipitation from May to October accounted for 88% of the whole year	There are three coal caves below the cliff, which were mainly exploited from south to north. Before the landslide occurred, coal mining activities lasted for 5 years
The Yudong landslide	Low-middle elevation karst mountainous valley landform	Maokou and Qixia Formation of middle Permian (P_2m+q): limestone intercalated with calcareous shale and micrite limestone; Liangshan Formation of lower Permian (P_1l): quartz sandstone, shale, bauxite and a thick coal seam with the thickness of 0.7 m	The strata occurrence is 315–320°∠3°–5°, two groups of dominant discontinuities are: J1: 284°∠85°, whose direction is almost parallel to the extension direction of cliff; J2: 39°∠84°, intersects with the extending direction of cliff	Karst features such as karst depressions and sinkholes are well developed. There is a sinkhole with a diameter of 17 m in at the top of cliff at 1# landslide. This sinkhole is connected with the steep crack at the back edge of collapse. There are other 16 sinkholes on the top of cliffs around the collapse area, the largest one has a diameter of more than 20 m, and the smallest one has a diameter of 5 m. The average annual precipitation is 1240.4 mm, and rainy season is from April to October, accounting for 84% of the whole year	The coal mine upstream of the collapsed began to exploit in 2006. The main shaft exit of the coal mine is 90 m away from the landslide, the excavation length is 900 m and the goaf area is $1.85\times10^4 m^2$

Table 2 (continued)

Landslides	Topography	Main lithology (from top to bottom)	Geological structure	Karst hydrogeology and rainfall	Mining activities
The Jiguanling landslide	Middle elevation karst mountainous landform	Changxing Formation of upper Permian (P_3c): limestone intercalated with flint limestone; Upper Wujiaping Formation of upper Permian (P_3w^2): shale intercalated siliceous at the top, the middle and lower sections are flint limestone intercalated shale; Lower Wujiaping Formation of upper Permian (P_3w^1): the upper section is composed of shale intercalated with micrite limestone and scattered pyrite; the middle section is a coal seam with thickness of 0.4–2 m; the lower section is composed of hydromica bauxite shale intercalated with carbon bauxite shale; Maokou and Qixia Formation of middle Permian (P_2m+q): limestone; Liangshan Formation of lower Permian (P_1l): bauxite shale with limestone	The strata occurrence is 295°–310°∠70°–80°, three groups of dominant discontinuities are: J1: 297°–315°∠67°–81°; J2: 32°–65°∠67°–87°; J3: 120°–140°∠63°–74°	Karst phenomenon is developed, there are many karst caves mainly developed in the limestone strata of Permian. The average daily maximum rainfall is 119.6 mm, and is mostly concentrated from May to September, accounting for about 62% of the total rainfall of the whole year	In 1992, Xinglong Coal Mine Company exploited 1100 m. The angle between the direction of tunnel and coal seam was about 25°. The mining method was shields mining. The coal mining face was arranged along the direction of coal seam, and the goaf was separated from the working space with the shield support. The stoping is connected to the main shaft of the Walnut tunnel through the air shaft. The Walnut tunnel was mined before the Xinglong tunnel, and the mining direction was from top of the mountain to the bottom

Table 2 (continued)

Landslides	Topography	Main lithology (from top to bottom)	Geological structure	Karst hydrogeology and rainfall	Mining activities
The Pusa landslide	Low–middle elevation mountainous landform with heavy erosion	Yelang Formation of lower Triassic (T_1y): limestone, silty mudstone and argillaceous siltstone; Changxing and Dalong Formation of upper Permian (P_3c+d): silty mudstone, limestone and argillaceous siltstone; Longtan Formation of upper Permian (P_3l): argillaceous siltstone, carbonaceous mudstone and coal seam	The strata occurrence is 170°∠5°–10°, three groups of dominant discontinuities are: J1: 100°–105°∠80°–90°; J2: 6°–9°∠80°–90°; J3: 140°–150° ∠80°–90°	Dissolution karst valleys and collapses are developed in the outcropping area of soluble rocks. Atmospheric precipitation is quickly poured into the ground to replenish groundwater through karst topography such as sinkholes and funnels. The average annual rainfall is 1200–1300 mm. The rainfall from May to September is concentrated, accounting for more than 70% of the total precipitation of the whole year	There are 6 mineable coal seams in this area, with a total thickness of 8.06 m and a mining area of 9.6×10^5 m^2. The mining adopts the strike longwall receding coal method, and the roof is managed by the collapse method
The Jiweishan landslide	Low-middle elevation karst mountainous landform	Maokou and Qixia Formation of middle Permian (P_2m+q): limestone with a layer of carbonaceous shale; Liangshan Formation of lower Permian (P_1l): hydromica clay containing thick hematite of 2 m; Hanjiadian Formation of upper Silurian (S_2h): silty shale	The strata occurrence is 345°∠21°–35°, two groups of dominant discontinuities are: J1: 185°∠75°, which is almost parallel to strata strike; J2: 77°∠80°, which is almost orthogonal to strata strike	The northern boundary has developed intensely karst phenomenon, forms a karst zone with many karst caves, and the western boundary is composed of a vertical karst crack with a nearly north–south trend. The average annual rainfall is 1111 mm, and rainfall is concentrated from April to September, accounting for 79% of the total annual precipitation	There is a large-scale goaf below the sliding body. The length of the goaf is 360 m and the width is about 137 m. Mining activities from 1960s was located below the key block, and after 2004 was outside the front edge of the sliding body
The Madaling landslide	Low-middle elevation karst mountainous landform with heavy erosion	Xiangbai Formation of lower Carboniferous (C_1x): quartz sandstone, sandy shale, carbonaceous shale and coal seams	The strata occurrence is 286°∠16°, two groups of dominant discontinuities are: J1: 30°∠85°; J2: 110°∠82°, these discontinuities constitute the back edge of the landslide	Karst landforms such as karst caves, sinkholes and cracks are well developed in this area, and karst water is stored in cracks and then transported. The average annual precipitation is 1446 mm. The rainfall is mostly concentrated from May to October, accounting for about 75% of the total rainfall of the whole year. June is the peak rainfall of the whole year	There are 4 coal seams below the landslide. The thickness of the A7 and A9 are thick, the mining height is 2.0–2.5 m, the mining footage is 200 m, and is mainly organized by local government. A10 and A11 are thin, mainly mined by local coal kilns, the mining height is 1 m, and mining footage is less than 100 m

Table 2 (continued)

Landslides	Topography	Main lithology (from top to bottom)	Geological structure	Karst hydrogeology and rainfall	Mining activities
The Zengziyan unstable zone	Two-level cliffs, and middle-high elevation mountainous landform with heavy erosion	Changxing Formation of upper Permian (P_3c): limestone; Longtan Formation of upper Permian (P_3l): breccia limestone; Maokou and Qixia Formation of middle Permian (P_2m+q): limestone, calcareous shale with limestone; Liangshan Formation of lower Permian (P_1l): carbonaceous shale, bauxite, and claystone; Hanjiadian Formation of upper Silurian (S_2h): silty shale	The strata occurrence is 290°–310°∠4°–11°, each unstable rock mass has 2–3 groups of dominant discontinuities	The vertical zoning of karst is obvious, and karst forms and distribution are different with different elevation. The second cliff is dominated by karst caves, and the contact surface between limestone and carbonaceous shale at the bottom of the first cliff is mainly characterized by karst springs. The average annual precipitation is 1185 mm	The bauxite of P_1l below Zengziyan Cliff was first mined in 1983, and the method of mining is mainly underground mining. Mined-out area is more than $2.88 \times 10^5 m^2$, covers the whole area of the second cliff of Zengziyan and the northwest side of the first cliff
The Wangxia unstable rock mass	Low-middle elevation karst mountainous landform with heavy erosion	Upper Wujiaping Formation of upper Permian (P_3w^2): siliceous and calcareous limestone intercalated with flint limestone; Lower Wujiaping Formation of upper Permian (P_3w^1): carbonaceous shale, siltstone, mudstone and coal seam; Gufeng Formation of middle Permian (P_2g): limestone, dolomite, siltstone, intercalated with a coal line of 5–20 cm	The strata occurrence is 335°–345°∠3°–8°, two groups of dominant discontinuities are: J1: 235°–255°∠75°–85°, J2: 150°–175°∠75°–85°. J2 in each rock mass are connected with each other, forming a plane with excellent extension and connectivity, and the plane is parallel to the failure surface of unstable rock mass	The karst phenomenon is relatively developed, and the karst morphology is mainly manifested as ground pits and dissolution cracks. The back edge of the rock mass extends along the karst funnel and is separated from the stable rock except the bottom. The annual average rainfall is 1049.3 mm, and rainfall is concentrated from May to September, accounting for 68.8% of the whole year	There are abandoned coal mines on the east and west sides of unstable rock mass, and there are also many small coal mines on the highway. The thickness of coal seam is only 5–20 cm; however, the nearest mining area is only 20 m away from the bottom of unstable rock mass

Table 2 (continued)

Landslides	Topography	Main lithology (from top to bottom)	Geological structure	Karst hydrogeology and rainfall	Mining activities
The Kaiyang landslide	Middle elevation karst mountainous landform with heavy erosion	Qingxudong Formation of lower Cambrian ($\in_1 q$): shale with sandstone; Mingxinsi Formation of lower Cambrian ($\in_1 m$): the middle and upper section is silty mudstone with quartz sandstone, and the lower section is silty mudstone; Jindingshan Formation of lower Cambrian ($\in_1 j$): the upper section is composed of sandy mudstone, clayey siltstone and clayey siltstone, the middle section is limestone intercalated with sandstone, and the lower section is sandy shale and argillaceous sandstone; Niutitang Formation of lower Cambrian ($\in_1 n$): carbonaceous mudstone intercalated with marl and 0–1.4 m phosphorite at the bottom; Dengying Formation of upper Sinian (Z_2dy): dolomite with shale at the bottom; Doushantuo Formation of lower Sinian (Z_1ds): phosphorite at the top and quartz sandstone at the bottom; Nantuo Formation of upper Nanhua (Nh_2n): shale, mudstone, silty slate, intercalated with a layer of moraine conglomerate	The strata occurrence is 105°–120°∠30°–48°, there are three dominant discontinuities in dolomite of Z_2dy: J1: 320°–340°∠65°–85°, forms the back edge of the collapse; J2: 185°–195°∠75°–85°, the maximum extension length is 50 m, and the connectivity is good, J3: 275°–280°∠45°–65°	Karst water mainly stores in the cracks of dolomite of Z_2dy and limestone of $\in_1 j$, and is mainly supplied by atmospheric precipitation. The annual average rainfall is 1132.4 mm, the annual average rainfall day is 205 days, and the rainy season is from May to September	There are six ore sections in the mining area, which have been mined since 1950s. The combined development scheme of multi adit central inclined shaft, strike long-arm mining method. Since the beginning of 1980s, the mining area has been in chaos, some of private coal mining activities have stolen pillars

Table 2 (continued)

Landslides	Topography	Main lithology (from top to bottom)	Geological structure	Karst hydrogeology and rainfall	Mining activities
The Xiaoba landslide	Low-middle elevation mountainous landform with heavy erosion	The first, second, third section of Dengying Formation of upper Sinian (Z_2dy^1, Z_2dy^2, Z_2dy^3) and the first section of Doushantuo Formation of lower Sinian (Z_1ds^1) are mainly dolomite; The second section of Doushantuo Formation of lower Sinian (Z_1ds^2): phosphorite; The third section of Doushantuo Formation of lower Sinian (Z_1ds^3): siliceous rock; The forth section of Doushantuo Formation of lower Sinian (Z_1ds^4): phosphorite; Nantuo Formation of upper Nanhua (Nh_2n): moraine conglomerate; Qingshuijiang Formation of Qingbaikou (Qbq): variable clayey siltstone, silty slate, tuffaceous siltstone with tuff	The strata occurrence is 100°–160°∠35°–60°, two groups of dominant discontinuities are: J1: 290°–335°∠46°–60°; J2: 205°–220°∠77°–88°	Karst is developed and karst groundwater is very rich. The average annual precipitation is 1135 mm, and the rainy season is from mid to late April to November, of which the rainfall is the most concentrated in April, May and June, accounting for 39.3–53.8% of the annual rainfall	The left slope toe is mainly underground mining, while the right slope toe is mainly open-pit mining. The right slope toe is excavated to form an open pit with a depth of about 60–80 m, a perimeter of about 520 m and an area of about 1.5×10^4 m^2

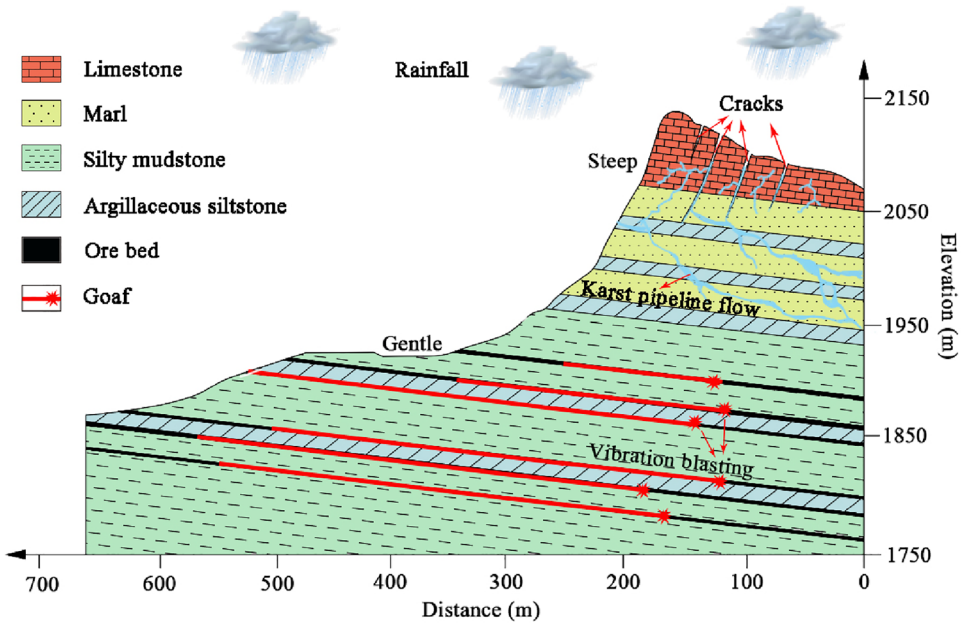

Fig. 2 Schematic diagram of the environmental characteristics for mining rockslides in the karst mountainous areas of southwestern China

thickness, which form a structure of soft–hard interbedding or hard–soft–hard interlayer with hard strata (Li and Wang 1994; Xu et al. 2016; Fan et al. 2019; Li et al. 2020a, b). The corrosion of soluble carbonate strata provides a seepage channel for water entering the soft interlayers and then softening the interlayers. Therefore, the soft interlayer usually plays an important role in controlling the occurrence of landslides (Yang et al. 2018).

Geological structure

Affected by the Yanshan Movement, folded mountains with a trend of NNE–NE is formed. Joints and cracks in the carbonate stratum are extensively developed, while two or three of them extend to be dominant discontinuities (Zhang et al. 2018). These discontinuities are generally an important factor in controlling the stability of the slope. The internal fillings in these discontinuities will dissolve during the rainfall and karst process (Detwiler and Rajaram 2007), then the water pressure and lubricate sliding surface appear in the potential sliding area, which will reduce the strength and integrity of rock masses with the process of extension induced by mining activities.

Karst hydrogeology and rainfall

There are many branches and intricate karst conduits in carbonate rocks in the karst mountainous areas of Southwest China (Fig. 3a), in which the strong effect of dissolution causes surface runoff, quickly leaking into sinkholes, dolines, and karst conduits (Fig. 3b) (Goeppert et al. 2011), forming an underground hydrological network. Affected by the subtropical monsoon climate, the annual precipitation in this area is mostly 800–1600 mm, of which summer precipitation accounts for about 70% of the annual precipitation. Abundant and intense rainfall in summer plays a crucial role in the induction of landslide in mountainous areas, especially in slopes with mining activities (Dahal and Hasegawa 2008; Martha et al. 2015). The influence of rainfall on slope stability is mainly reflected in three aspects: physics, chemistry, and mechanics. In terms of physical effect, intense and continuous rainfall leads to rapid rise of groundwater level, which could not only produce high-pressure air mass on the upper section of karst conduits cavity and lead to karst collapse (Jiang et al. 2017), but also soften rock masses, resulting in significant reduction of physical and mechanical properties. For chemical effect, the chemical ions contained in rainwater would be dissolved or exchanged with the rock mass, resulting in changes in the composition or structure of the rock mass (Li et al. 2020a, b). The mechanical effect mainly includes hydrostatic pressure and hydrodynamic pressure. Hydrostatic pressure refers to the thrust generated by rainfall through vertical discontinuities on the trailing edge of the slope and the uplift pressure generated on the potential sliding surface (Wu et al. 2010). Hydrodynamic pressure is the outward seepage force borne by karst conduits, which is caused by the head difference between the front and rear edges of the slope due to rainfall (Gu et al. 2017), aggravating deformation of the slope. In addition, rainfall is often coupled with mining-induced fractures, which intensifies the expansion of fractures and

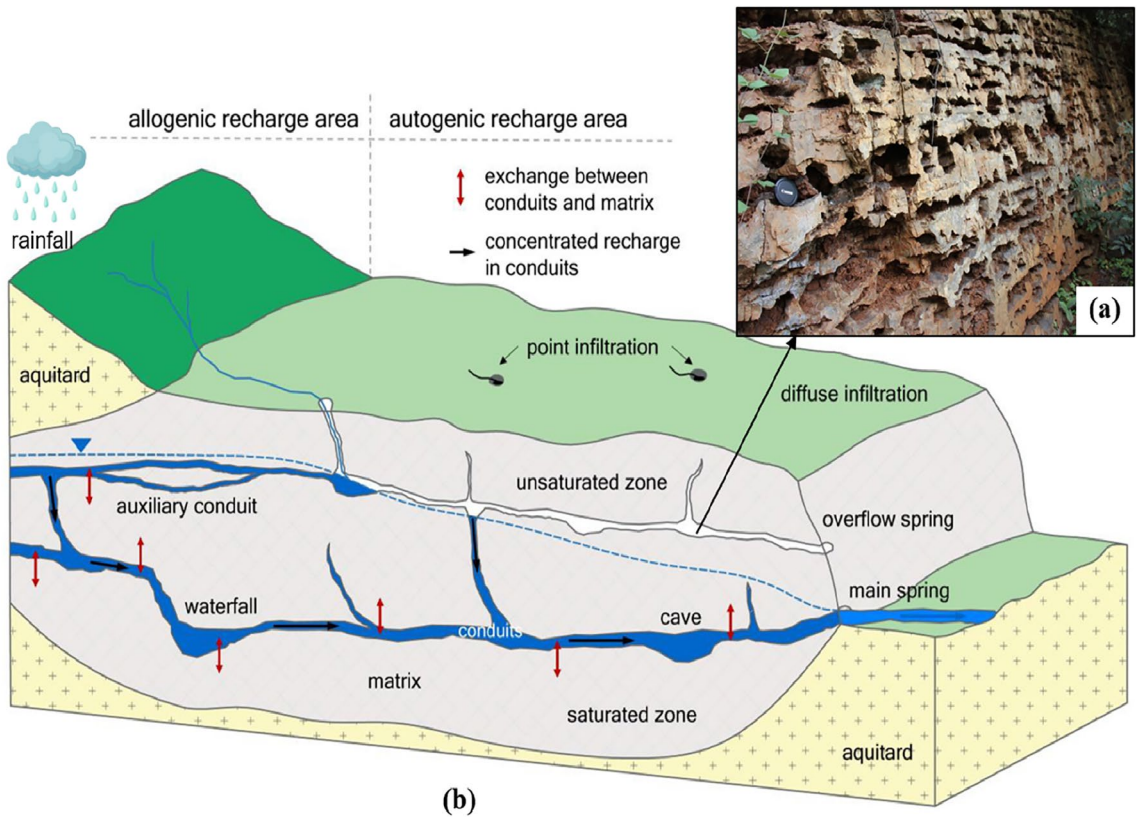

Fig. 3 Karst hydrogeology in southwestern China. **a** Karst conduits in rock masses; **b** geological concept model of karst conduits system (Li et al. 2021)

becomes the triggering factor for landslides (Xiong et al. 2021).

Mining activities

Mineral development projects in Southwest China are one of the pillar industries because of its superior geological conditions, abundant mineral resources and considerable output. As many as 12 ore-bearing strata have been discovered in this area, of which the main mining strata are Liangshan Formation (P_1l) and Longtan Formation (P_3l) of Permian, and Doushantuo Formation (Z_1ds) and Dengying Formation (Z_2dy) of Sinian. The thickness of ore strata is generally thin (Fig. 4a), mostly between 0.2 and 1.5 m.

The impacts of mining activities on slopes can be divided into direct and indirect. The direct impacts are that decades or even hundreds of years of manual or mechanical mining activities in these mining areas have formed enormous underground or open-pit goaf. The goaf causes the falling of the roof, the bending and settling of the overlying strata, and the formation of many deep and large ground cracks on the surface (Xia et al. 2016). These large mining-induced ground cracks will form the trailing edge of the landslide or a potential sliding surface, separating landslide masses from the stable slope. In addition to the formation of ground cracks, the existence of underground goaf will cause obvious deformation on the slope surface (Fig. 4b) and even induce large-scale regional horizontal movement (Li et al. 2009; Chen et al. 2021). Besides, the modern mining method of blasting also greatly affects the stability of the slope, especially in the generation of periodic tension–compression and shear effects, significantly reducing the shear strength of joints and the tensile–shear and compression–shear of rock masses (Ali et al. 2018; Cui et al. 2022; Li et al. 2022), which easily produce compression, tension and shear damage of key blocks, and then induce the formation of the rupture surface. The indirect impact of mining activities is that the above direct impacts cause mining-induced cracks and slope deformation, which further changes the karst landform and aggravates the development of groundwater channels. Mining cracks produce higher hydraulic conductivities and flow velocities, resulting in an increase of rock dissolution rate, which further increases the width of cracks and velocity of flows (Zhang and López 2019).

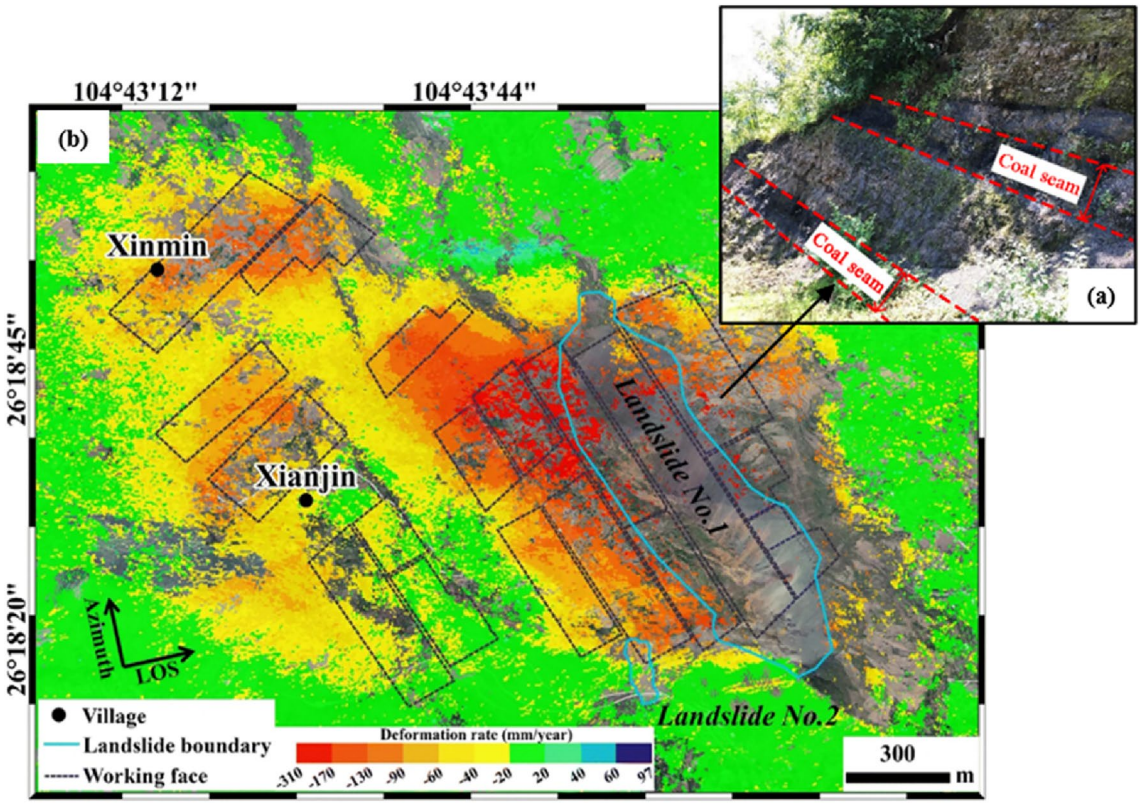

Fig. 4 Mining activities in southwestern China. **a** Thin coal seam; **b** deformation monitoring of mining-induced Jianshanying landslide (Chen et al. 2021)

Formation mechanism and failure mode classification system for mining landslides

The failure mechanisms and modes are related to slope structure types. According to the angle between strata inclination and slope inclination (β), Liu et al. (1993) classified the layered slopes into five types: subhorizontal bedding layered slope, bedding layered slope, anti-dip layered slope, lateral layered slope, and oblique inclined bedding layered slope. The bedding slope and anti-dip slope were classified into steep slope ($\alpha > 45°$), medium slope ($20° < \alpha < 45°$) and gentle slope ($10° < \alpha < 20°$) based on the dip angle of strata (α) (Fig. 5). In view of the above classification of slope types, as well as the Varnes landslide classification system (Varnes 1978) adopted by International Geotechnical Society's UNESCO Working Party on World Landslide Inventory (WP/WLI 1990), the updated system of Varnes (Hungr et al. 2014) and a special failure mode, which did not involve the Varnes and Hungr system (Yin et al. 2011). This paper systematically studies the mechanisms and failure modes for typical mining landslide with different slope structure types in karst mountainous areas of southwestern China and establishes a unified failure mode classification system for mining landslides.

Subhorizontal bedding layered slope

The subhorizontal bedding layered slope is a gentle slope whose dip angle is less than 10°. Controlled by topography and stratigraphic structure, subhorizontal bedding layered slopes are generally not prone to being destroyed. However, large-scale discontinuities at the crown of slopes provide initial favorable conditions for landslides. In the southwest mountainous area of China, most of the subhorizontal bedding layered slopes are in the core area of the folds and are not affected measurably by folds. But there exist many steeply dipping 'X-shaped' discontinuities, which detach unstable rock masses from intact slopes (Poisel et al. 2009). These unstable rock masses always 'tower shaped' or 'slab shaped' with a remarkable height–diameter ratio. The typical failure modes of this kind of slope are generally rock rotational slide, rock block topple and rock collapse owing to the influences of karst hydrogeology, rainfall and mining activities (Rohn et al. 2004; Poisel et al. 2005; Hungr et al. 2014).

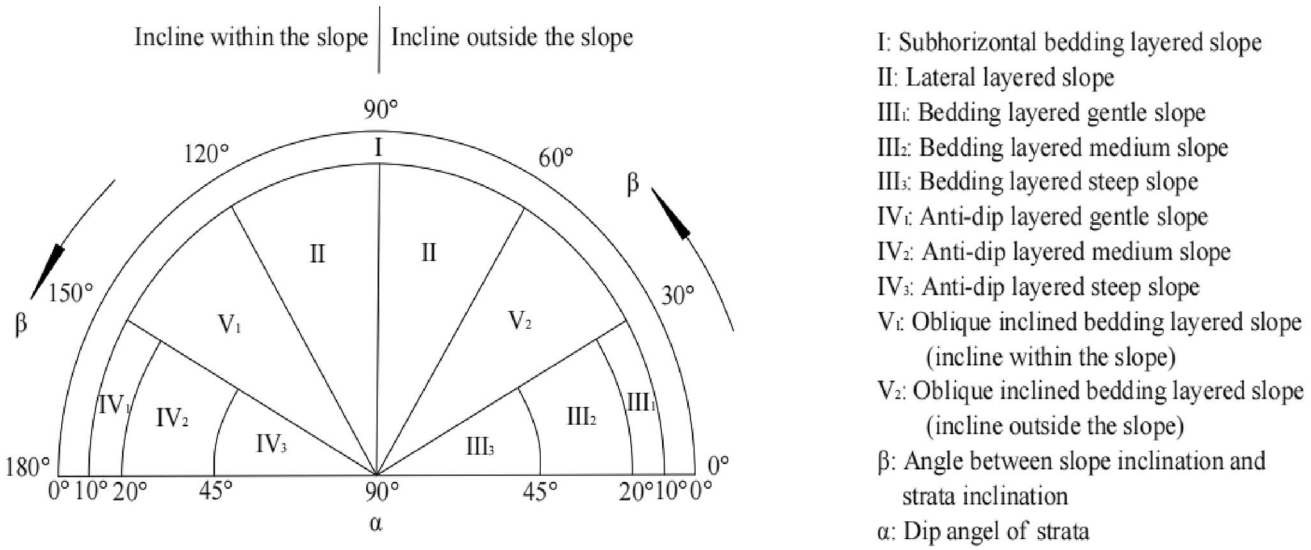

Fig. 5 Classification of slope structure types (Liu et al. 1993)

Rock rotational slide

Rock rotational slide ("rock slump") refers to masses sliding along a rotational rupture surface, while the underlying strata of the sliding masses are always soft layers. The formation process of the rotational potential surface is that discontinuities at the crown of the slope continues extending and the frontal edge of the slope creeps due to weak layers (Di Maggio 2014), which leads to a non-linear potential sliding surface. Before the rupture surface forms, the middle of the slope can be regarded as a 'locked segment' to prevent landslide (Huang 2015). In the mining area of southwestern China, rock rotational slide is one of the most common types of landslides. Widespread mine-out areas inside the slope lead to bending and subsidence of the overlying strata, while the upper part of the unstable rock mass moves inward the slope, and the toe of the slope moves toward the free surface owing to the influences of goaf and blast unloading effects. These effects exacerbate extrusion of the frontal edge and increase extending of large-scale discontinuities. Besides, karst water and mining cracks aggravate the crack propagation of locked segment, which leads to the formation of the whole rupture surface.

The unstable rock mass W2-2 at Wangxia Cliff of the Three Gorges area suffered rock rotational slide on October 21, 2010. Before sliding, W2-2 was a huge unstable rock mass about 80 m in length, 10–15 m in thickness and 70 m in height, with a volume of about $7\times10^4 m^3$ (Hu et al. 2019). The cliff in which W2-2 is located has a typical upper-hard and lower-soft lithology. The upper section of the Wujiaping Formation (P_2w^2), composed of hard rock, is located at the top of the cliff, while the lower section of the Wujiaping Formation (P_2w^1) is located at the bottom. Shale, siltstone, mudstone and coal seam in P_2w^1 compose a soft base with a thickness of about 14 m. The soft base has an obvious squeezing phenomenon under the persistent gravity of hard rock. Two large-scale discontinuities T16 and T12 constitute the boundary of W2-2 (Fig. 6a). Long-term mining activities below W2-2 resulted in an underground goaf of 2.4×10^5 m^2, which led to uneven subsidence and accelerated expansion of the two discontinuities. Besides, the rainfall on October 10–13 played an important role in seeping into cracks and increasing horizontal thrust and shear stress (Moosavi et al. 2016). On October 20, the maximum value of daily displacement of T12 and T16 was 22 mm and 80 mm (Sun et al. 2017), and on October 21, T16 accelerated its expansion upward. After that, W2-2 squeezed out from the soft base, then rotated, slid, and leaned on the stable slope (Fig. 6b). In addition to W2-2, there are 15 other unstable rock masses such as W29-1 and W29-2 at Zengziyan Cliff that have a similar failure mode to W2-2.

The failure process of the subhorizontal bedding layered slope with rock rotational slide affected by mining activities in the karst mountainous areas of southwestern China is shown in Fig. 6c. (1) The original unstable rock mass has a large-scale steeply dipping discontinuity and a soft base which is creeping. (2) Uneven mining settlement induces the unstable rock mass moving backward, pushing the slope toe to extrusion. Mining cracks are widely distributed, weaken the locked segment, connect with the discontinuity, and collect rainfall and karst water. (3) In the locked segment with brittle fractures, rotational slide occurs.

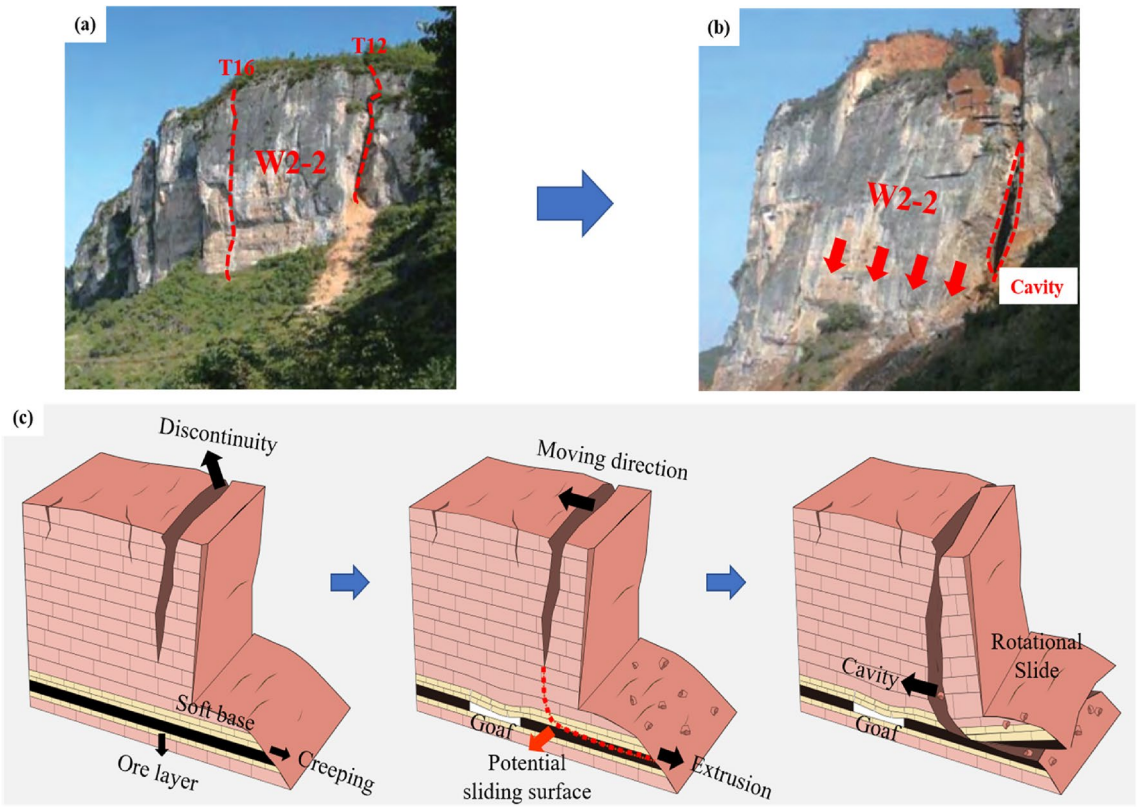

Fig. 6 Mining-induced rock rotational slide in subhorizontal bedding layered slope. **a** Unstable rock mass W2-2 at Wangxia Cliff (Huang et al. 2018); **b** failed rock masses (Huang et al. 2018); **c** schematic diagram of failure process

Rock block topple

Rock block topple refers to masses rotating outward around a point and then toppling. The point is usually at the bottom of an unstable rock mass. Different from 'rock flexural topple', rock block topple is more like a brittle failure which happens owing to increasing of overturning moment (Goodman and Bray 1976). In general, the overturning moment is controlled by increased water pressure in discontinuities at the crown of the slope, but in mining area of southwestern China, the positions of goaf and karst dissolution also lead to toppling. When the position of goaf is in the front of an unstable rock mass, the slope toe sinks and the discontinuities cause continuous downward tension (Ban et al. 2021) and instability and toppling of the unstable rock mass. Also, the dissolution of karst water plays a role in corrosion the rock nearby discontinuities, which accelerates detachment from the stable slope.

The Yaoyanjiao toppling at Houchang, Weining, and Guizhou Province is a typical failure mode of rock block topple in subhorizontal bedding layered slope, which occurred on January 27, 2006, with a volume of about 3.2×10^4 m^3. Before toppling, the unstable rock mass was at the Yaoyanjiao Cliff of Guizhou Plateau, which had an excellent free face on the south side. The upper cliff consists of medium–thick limestone, while the lower is quartz sandstone intercalated with a minable coal seam whose thickness is about 0.7 m. A longitudinal karst discontinuity cuts the unstable rock mass into a shape of thick slab, and the dissolution can be clearly seen in Fig. 7a. Besides, there was a huge karst cave with a width of more than 20 m and a maximum depth of 3 m below the slab-shaped rock mass. Both the karst discontinuity and the cave separated most part of the slab-shaped rock mass from the stable cliff, while only the bottom was connected. By the time the block toppling occurred, continuous mining activities had been conducted under the cliff for more than 5 years, and more than 75% of the coal seam had been exploited. Long-term open-stope mining method only relied on the self-supporting capacity of coal pillars and goaf roof. When the roof of goaf could not support the upper strata, the roof collapsed and the overlying layers were abscised, causing different downward tendencies for the overlying strata. The original stress varied and concentrated especially at the toe of slope, which increased the density of the cracks and reduced the ultimate tensile strength of the rock mass, making the unstable rock mass destructible. In addition, the original karst discontinuity extended downward and further decreased

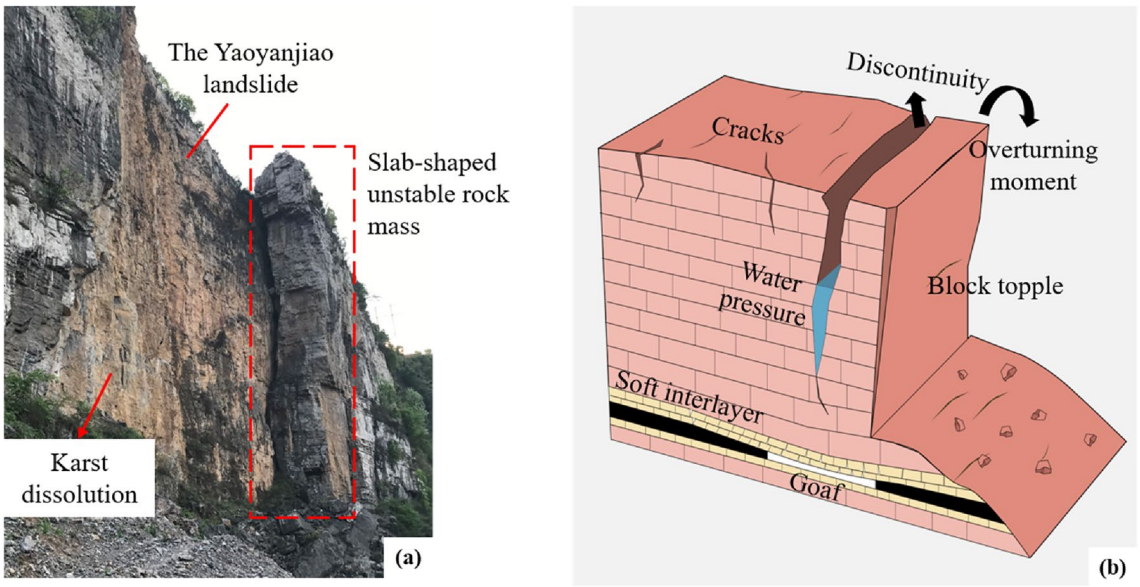

Fig. 7 Mining-induced rock block topple in the subhorizontal bedding layered slope. **a** The Yaoyanjiao landslide; **b** schematic diagram of the failure mode

connection with the cliff with the influence of underground mining. Eventually, the slab-shaped rock mass rotated outward around a point at the bottom and then toppled. After that, another slab-shaped unstable rock mass with a length of nearly 100 m remained on the west side of the toppled one and had a similar trend of block topple with it according to field investigation (Feng 2013). Besides, the Yudong 2# toppling at Longchang, Kaili, Guizhou and the prediction failure mode of 56 unstable rock masses at Zengziyan Cliff and unstable rock mass W1 at Wangxia Cliff were also a result of rock block topple.

The subhorizontal bedding layered slopes with failure modes of rock block topple induced by mining activities in the karst mountainous areas of southwestern China have the following characteristics: (1) steeply dipping discontinuities that separate unstable rock mass from stable slope exist; (2) the bottom of the unstable rock mass is far away from the weak interlayer, or is almost not affected by the weak interlayer; (3) mining position below the unstable rock mass is mostly in the front of the slope; (4) karst dissolution and rainfall have a strong effect in large-scale discontinuities. The failure mode of rock block topple is shown in Fig. 7b.

Rock collapse

Rock collapse ("rock irregular slide") refers to sudden or even rapid sliding on an irregular rupture surface consisting of randomly oriented joints, separated by segments of intact rock (Hungr et al. 2014). The failure mechanism of rock collapse is complex and may differ from each other because of different geological conditions. He et al. (2019b) described one of the failure processes as brittle fragment at the bottom of the unstable rock mass and collapse of the upper part, which can also be defined as bottom-fragment collapse. Different from the impact on rock rotational slide, the impact of mining activities on rock collapse is more reflected in the deterioration of compressive strength of the bottom rock masses rather than the shear strength, which may be related to dense cracks or low strength of the original rock mass (Li et al. 2018).

The typical cases include the Yudong 1# collapse in Kaili and the unstable rock mass W12 at Zengziyan Cliff (Fig. 8a). These two collapses have some common features. (1) Both have a steeply dipping dominant discontinuity, which has a high dissolution penetration rate, but less rock bridge: the rock bridge coverage area of the Yudong 1# discontinuity is less than 30% (Feng et al. 2014), and the penetration length of W12 discontinuity is 159 m and only 38.2 m is unpenetrated. (2) There are long-term mining activities below the unstable rock mass: the goaf below Yudong 1# collapse is $1.85 \times 10^6 m^2$, and the exit of the main tunnel is only 90 m away from the collapse. The coal seam of Longtan Formation (P_3l) in Zengziyan area was first mined in 1983, and legal and illegal mining activities excavated most of the coal in recent 20 years. (3) At the bottom of the unstable rock mass, weak layers, easily broken by mining blasting vibration, exist: The Maokou and Qixia Formation (P_2m+q) locates below the Yudong 1# collapse, in which the limestone is intercalated with multiple layers of calcareous shale, while the bottom of W12 is thick carbonaceous shale stratum, containing fragile rock.

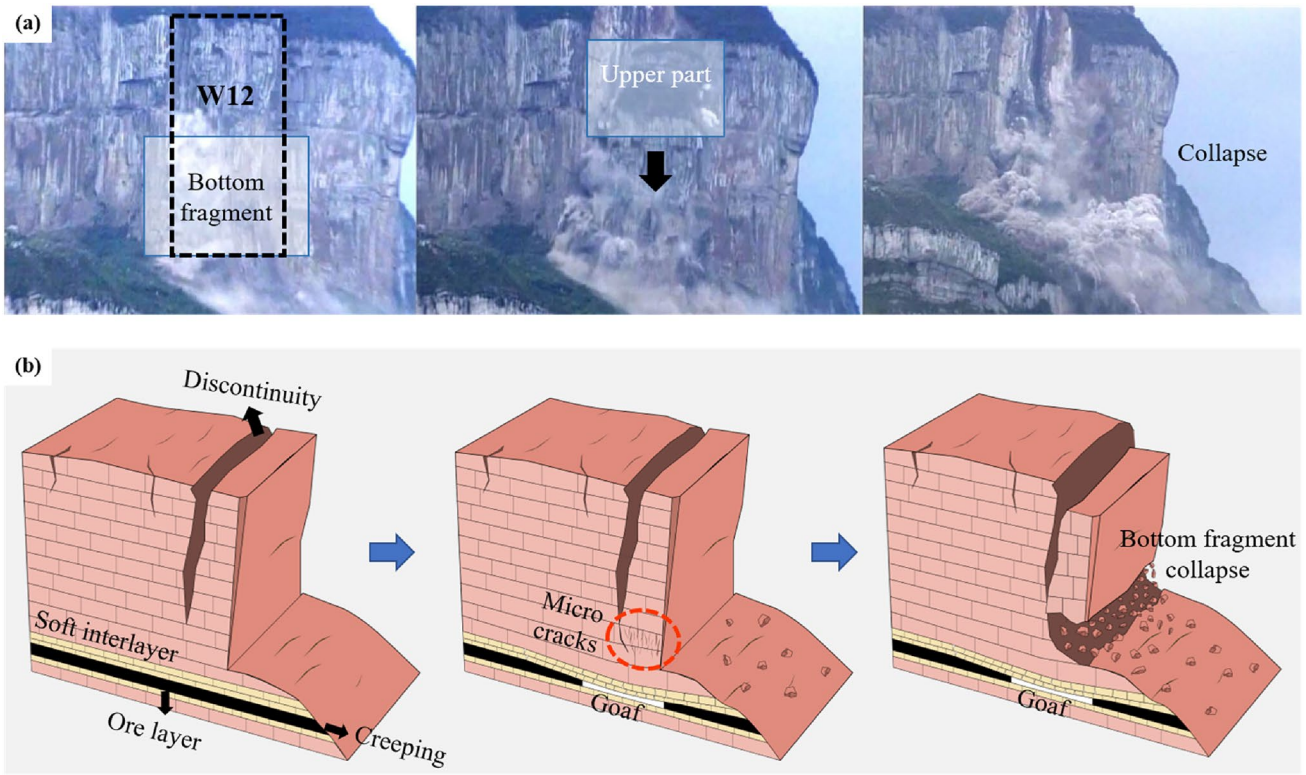

Fig. 8 Mining-induced rock collapse in the subhorizontal bedding layered slope. **a** Bottom-fragment collapse process of unstable rock mass W12 in the Zengziyan Cliff (He et al. 2019b); **b** schematic diagram of failure process

The formation process of bottom-fragment collapse induced by mining activities in the karst mountainous areas of southwestern China is shown in Fig. 8b. The original unstable rock mass has adverse geological conditions (e.g., steeply dipping discontinuities, easily broken weak layers, dense cracks). Mining goaf and karst dissolution lead to further extension of large discontinuities, and blasting vibration produces more microcracks or makes the existing microcracks connect with each other. When the microcracks at the bottom of the rock mass further develop into macrocracks, unable to bear the upper load, brittle fragmentation occurs and then the upper rock mass immediately collapses downward.

Bedding layered slope

Bedding layered slope is a kind of slope whose inclination is roughly the same as that of strata. The destructive proportion of bedding layered slope is much greater than that of other slope types. The failure mode of bedding layered slope is generally rock planar slide ("translational slide"). Rock planar slide refers to masses slide along a planar rupture surface, which is usually the bedding. The hard strata and soft strata have different mechanical properties, causing differential weathering and creeping along the bedding, in a favorable geological environment for planar slide. Continuous creeping results in cracking at the back edge. Thus, the front of the slope undertakes a locked segment to maintain stability. When the locked segment fails, the landslide body slides along the potential planar surface. Some of the scholars like Hu et al. (2018) also generalized this type of failure as progressive slide. However, mining action changes the stress of the slope and concentrates stress at the front of the slope, if the mineral is on the front of slope which is the worst-case scenario, the excavation will destroy the locked segment and accelerate the movement of subsequent masses. Even if the mining activities are not located at the front edge, the vibration waves and differential settlements will also deliver to the overlying strata and cause ground movement. Karst water and rainfall gathering through cracking at the back edge also lubricate the potential sliding surface and increase the sliding force.

The Xiaoba slide in Fuquan, Guizhou, with a total volume of 1.41×10^6 m^3 is a typical rock planar slide induced by mining in the karst mountainous areas of southwestern China (Yu et al. 2020a, b). The engineering geological profile is shown in Fig. 9a. This slope has a typical structure of hard–soft–hard interlayer. The strength difference between the overlying high-strength hard strata and the underlying low-strength strata is obvious. Among the soft formations,

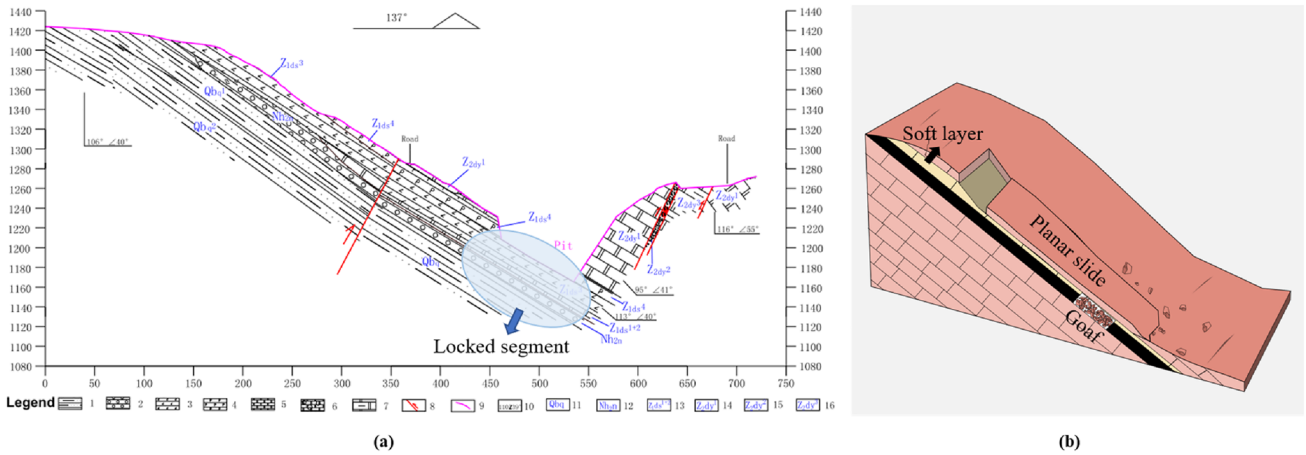

Fig. 9 Mining-induced rock planar slide in the bedding layered slope. **a** Engineering geological profile of the Xiaoba slope. 1 Clayey siltstone; 2 conglomerate; 3 silicalite; 4 phosphorite; 5 dolomite; 6 fragmental dolomite; 7 clayey dolomite; 8 reverse Fault; 9 terrain line before landslide; 10 occurrence; 11 Qingshuijiang Formation; 12 Nantuo Formation; 13 Doushantuo Formation; 14, 15, 16 Dengying Formation (Lin et al. 2018); **b** schematic diagram of the failure mode

the strength of clay siltstone in Qingshuijiang Formation (Qbq) is the smallest, and there is a strength interface between clay siltstone and the underlying silty slate, which constitutes a potential sliding surface. With long-term evolution, differential sliding phenomenon of the two strata led to the formation of tensile cracks at the rear edge of the slope and a locked segment at the front edge of the slope. The locked segment became a key area for controlling the stability of the slope. However, as open-pit mining and underground mining were carried out at the front edge of the slope, the thickness of the key phosphorus rock masses that acted as the locked segment decreased, and stress was further concentrated on the remaining phosphorus masses. When stress was concentrated to a limit, the locked segment was brittly sheared, producing a rock planar slide. In addition, rainfall lasted for 1 month before landslide, and the rainfall during the month of landslide was 100–200 mm, which means rainfall also has a triggering effect in the Xiaoba slide (Xing et al. 2016).

The bedding layered slopes with failure mode of the rock planar slide induced by mining in the karst mountainous areas of southwestern China generally have the following characteristics: (1) soft–hard interbedding or hard–soft–hard interlayer form a potential sliding surface along the bedding; (2) mining activities in the locked segment greatly damage the slope stability, while mining below the sliding surface accelerates downward sliding; (3) rainfall gathers through cracking at the back edge into potential sliding surfaces. The failure mode of rock planar slide is shown in Fig. 9b.

Anti-dip layered slope

Anti-dip layered slope refers to a layered slope whose strike is almost the same as that of the strata, but the inclination is opposite (Xie et al. 2015). It is generally believed that this type of slope is more stable than bedding layered slope, and it is less prone to instability. However, in recent years, engineering geological problems of anti-dip layered landslides caused by mining have frequently occurred, triggering close attention.

Anti-dip layered gentle slope

Anti-dip layered gentle slope is widely distributed in the karst mountain area of southwestern China; the dip angle of this kind of slope is relatively gentle ($10° < \alpha < 20°$). As the stratum inclines inside of the slope, there will be no slide along the bedding, but is mainly controlled by dominant discontinuities. Generally speaking, the failure mode in the anti-dip layered gentle slope is similar to the failure process in the subhorizontal bedding layered slope, that is, rock rotational slide, which experiences the process of 'trailing edge cracking–frontal edge creeping–middle segment locking' and middle segment shearing. Mining activities promote effectively the expansion of trailing edge fractures and weaken shear the strength of locked segment rock masses.

The typical cases induced by mining activities in the karst mountainous areas of southwestern China are Pusa landslide (Fig. 10a) in Nayong of Guizhou (Fan et al. 2019), Faer landslide in Shuicheng of Guizhou (Yu et al. 2020a, b), and Madaling landslide in Duyun of Guizhou (Zhao et al. 2016). The failure mode is shown in Fig. 10b.

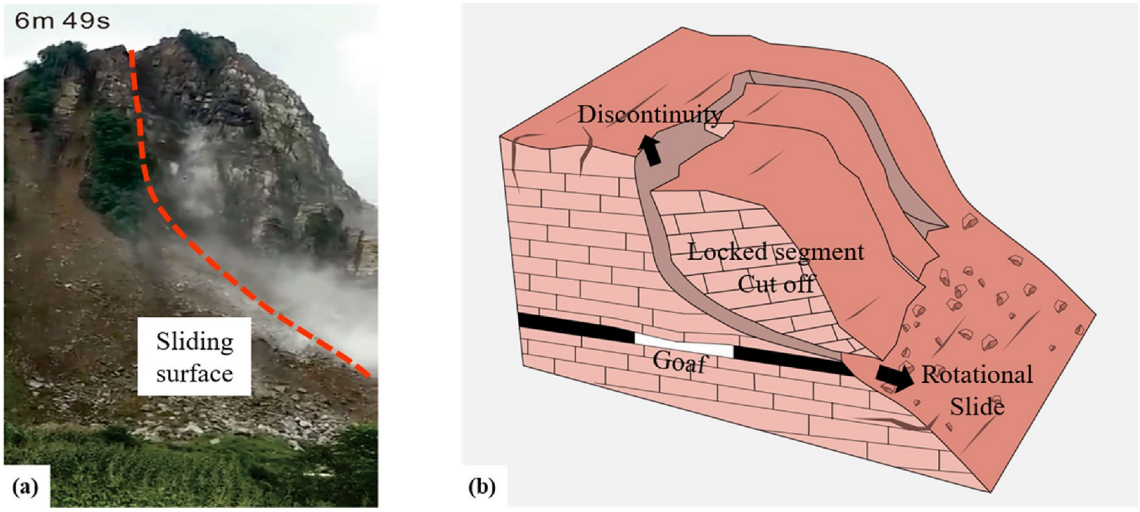

Fig. 10 Mining-induced rock rotational slide in anti-dip layered gentle slope. **a** The Pusa landslide (Fan et al. 2019); **b** schematic diagram of failure mode

Anti-dip layered steep slope

Anti-dip layered steep slope is a type of steep slope with a dip angle of more than 45°. This kind of slope is prone to damage owing to gravity, which is defined as toppling by Freitas and Watters (1973). Goodman and Bray (1976) defined this type of failure as 'rock flexural topple' to make a distinction with 'rock block topple'. In the natural environment, flexural toppling strata can be regarded as cantilever beams, which would bend. When each rock beam reaches tensile strength, it would produce fractures, and then toppling happens along the rupture surface formed by fractures of rock beams. Induced by mining activities, the secondary flexural topple is a key reason for aggravating the velocity and degree of anti-dip layered steep slope while supplemented by bending of gravity (Hoek and Bray 1981), whether it is open-pit mining or underground mining. In mechanics, the mechanism of failure caused by open-pit mining and underground mining is not completely the same. Open-pit mining usually begins at the foot of the slope. Owing to that a new space for flexural topple is produced, while the overlying strata loses effective support and bends toward the goaf. When rock beams reach ultimate tensile strength, they fracture and form a rupture, and then topple to create a disaster. More studies have shown that while most of the overlying rock beams suffer toppling, there might be some shearing of rock beams (Xie et al. 2019). As for underground mining, the goaf is located inside the slope. After mining, the toppling process of the overlying strata is accompanied by roof caving and bending of the overlying strata, which is a more composite failure process. In the case of the same mining length, the fracture depth of the overlying strata in underground mining might be greater; thus, the depth of the rupture surface might be deeper. Once damaged, the volume of landslide is greater, resulting in harmful disaster. In addition to mining activities, karst and rainfall also impair anti-dip layered steep slopes. When the dip angle of the steep slope is large, rainfall is easier to flow into the deeper slope along the steep bedding, which not only increases staggering of rock beams, but also produces fragmented rock masses.

The flexural toppling of Honglianchi iron mine in Hefeng, Hubei Province is a typical mining case of the anti-dip layered steep slope in the karst mountainous areas of southwestern China Fig. 11a. It was induced by both open-pit and underground mining, and the volume was about 2.5×10^4 m^3. The original slope is mainly composed of limestone, iron and quartz sandstone, while iron is in the middle of slope. The early mining activity was open-pit mining and the excavation was along the direction of bedding, forming a huge pit with a length of 115 m, a width of 18 m and a height of 20 m (Wang et al. 2014). The pit provided a deformable bending space for the overlying strata and formed some tensile cracks. Afterward, the mining method was changed to underground, and horizontal mining was carried out through two mines. This kind of mining method aggravated the connection of the rupture surface, and finally the overlying strata toppled. However, the range of mining area is not so large, while there is a thick 'key block' underlying the iron stratum, which increases flexural rigidity and sliding resistance. Therefore, the volume of toppling was not so big and only the upper suspended masses toppled. The failure mode is shown in Fig. 11b.

The anti-dip layered steep slopes that suffer flexural topple due to mining activities in the karst mountainous areas of southwestern China have the following characteristics: (1)

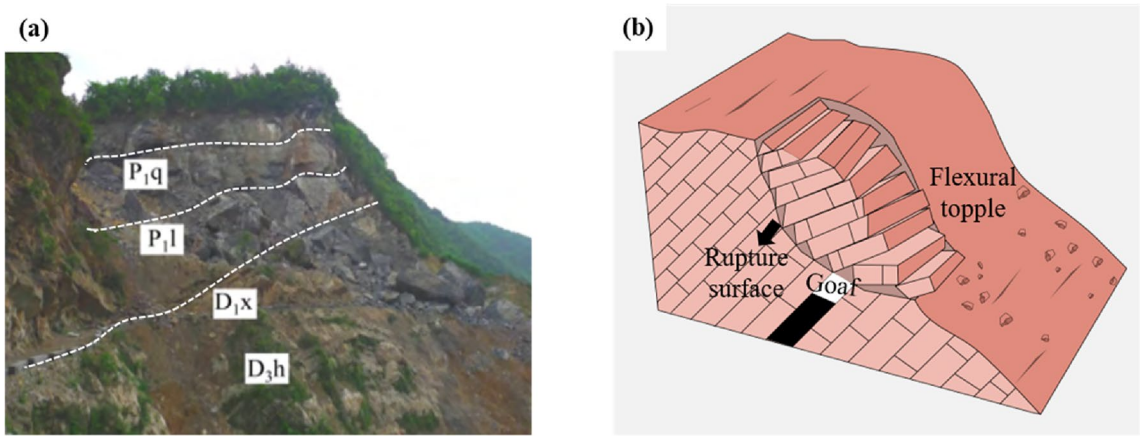

Fig. 11 Mining-induced rock flexural topple in anti-dip layered steep slope. **a** The Honglianchi landslide (Wang et al. 2014); **b** schematic diagram of failure mode

the original rock beams, in nature, present flexural bending due to self-gravity; (2) open-pit mining creates a deformable space for flexural topple, while underground mining causes a composite failure of flexural topple and shear sliding; (3) rainfall flows into deeper slope through steeply dipping beddings.

Lateral layered slope

Lateral layered slope is a type of slope whose inclination is perpendicular to strata inclination. Studies on the mechanism and failure mode of this kind of slope are far less than those on other types of slopes because of their naturally good stability. However, the lateral layered steep slopes generate failure of flexural topple like the anti-dip layered steep slopes, and the damage maybe more harmful than the anti-dip layered steep slopes because of the condition of three free faces. That means once flexural topple occurs, rock avalanche will happen along two directions of inclination and strike.

The typical case is Jiguanling landslide in Chongqing (Fig. 12a). The original slope was a steep triangular prism, which produced good free-face conditions in the north, east and west. The mining method is underground mining with the maximum mining depth of 1100 m, and eventually the original coal pillars were also mined out. Different from Honglianchi slope, the underlying strata of Jiguanling slope is thinner, which is only about 60 m and is not enough to support overlying rock mass. Finally, the lower rock masses sheared and slid, while the overlying rock layers broke and toppled, causing a two-direction catastrophic landslide. This case also demonstrates that the thickness of the underlying strata might be crucial for the volume of the landslide. The thicker the underlying strata,

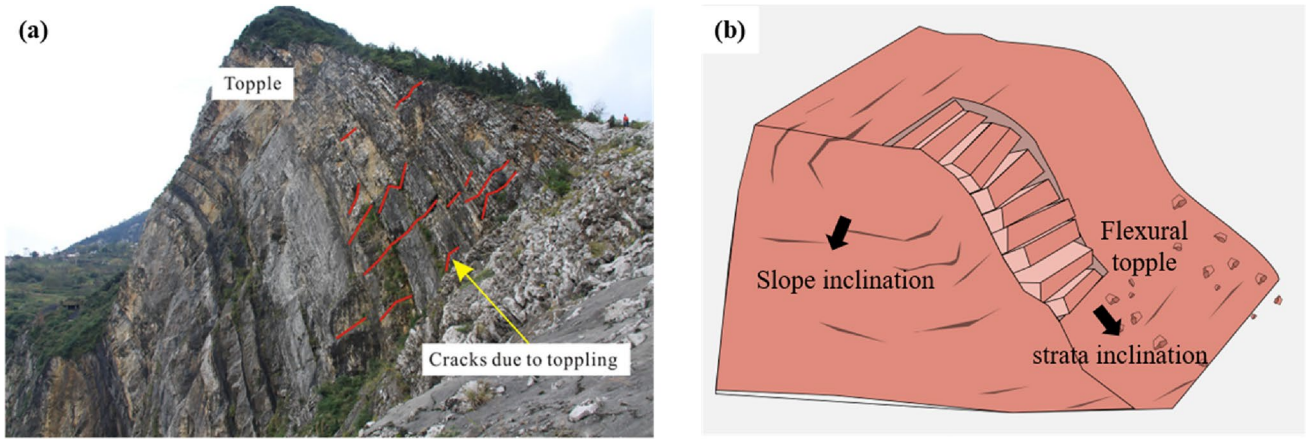

Fig. 12 Mining-induced rock flexural topple in lateral layered slope. **a** Flexural topple phenomenon in Jiguanling (Li et al. 2016a, b); **b** schematic diagram of failure mode

the more difficult it is to be damaged by shear (Vanneschi et al. 2019). The failure mode is shown in Fig. 12b.

Oblique inclined bedding layered slope

According to the classification of slope structure types (see Fig. 5), two kinds of oblique inclined bedding layered slopes exist, one inclined outside the slope and the other inclined within the slope. The failure mode of the former ones is similar to that of the bedding layered slope, that is, rock planar slide along the bedding plane (Fig. 13a). However, because there is a certain angle between strata inclination and slope inclination in oblique inclined bedding layered slope, planar slide looks more like a slide from the lateral side of the slope. The inclined inside ones suffer a failure mode of apparent dip slide (Fig. 13b) (Yin et al. 2011) that refers to rock masses sliding toward the direction of apparent dip due to the deformation limitation of the true dip. The occurrence of this kind of landslide is mainly affected by terrain and other environmental factors, but the effect of underground mining like mine-out and blasting causes a landslide ahead of time.

The segment of cracks T8–T12 of Lianziya Cliff in the Three Gorges and the Jiweishan slide (Fig. 13c) in Chongqing are typical cases of apparent dip slide induced by mining in the karst mountainous areas of southwestern China. There are many similarities in topography, mechanism and other aspects, which can be summarized as the following five aspects. (1) Creep slowly along the weak layer due to long-term underground mining activities: the unstable rock mass in Lianziya Cliff has four weak layers and creeps along each weak layer. The Jiweishan slope mainly slides along the weak intercalation of carbonaceous shale in Maokou and Qixia Formation (P_2m+q) (Xu et al. 2010). (2) Vertical discontinuities cut the sliding mass from stable slope: in the past 100 years, Lianziya Cliff formed many cracks induced by mining activities, cutting the rock mass into blocks. The south and west sides of Jiweishan slope formed two perpendicular dissolution cracks induced by nearly 10,000 years of karst dissolution (Kulatilake and Ge 2014). (3) A stable slope in the direction of true dip, limiting deformation of sliding rock masses: in the direction of true dip, the unstable rock mass in Lianziya leans on stable cliff, and the Jiweishan slope has a good integrity in true dip, which can effectively prevent the rock mass from sliding. (4) The free-face condition is well in the direction of apparent dip: the north and east sides of Lianziya Cliff are free faces (Zuan and Huang 2018), and the apparent dip direction of the Jiweishan slope is deeply cut by river, which provides favorable conditions for the apparent dip slide. (5) Mining activities are frequent below the slope: after about 443 years of mining activities below the Lianziya Cliff, a goaf of about 1.2×10^5 m^2 was formed. The Jiweishan slope formed a large-area goaf at a depth of 78 m below the front edge of the sliding rock masses, which affected the stability of the slope. The failure mode of the apparent dip slide is shown in Fig. 13b.

Mechanical model and stability criteria

To study the formation mechanisms and failure modes for mining-induced landslides, scholars proposed mechanical models for the failure mode of rock flexural topple and rock planar slide, respectively, and the corresponding stability criteria were put forward, which could analyze failure mechanism from the perspective of mechanics and judge the stability of slopes.

Cantilever beam limit equilibrium model for rock flexural topple

Cantilever beam limit equilibrium model for rock flexural topple is suitable for anti-dip layered and lateral layered steep slopes induced by open-pit mining activities. The

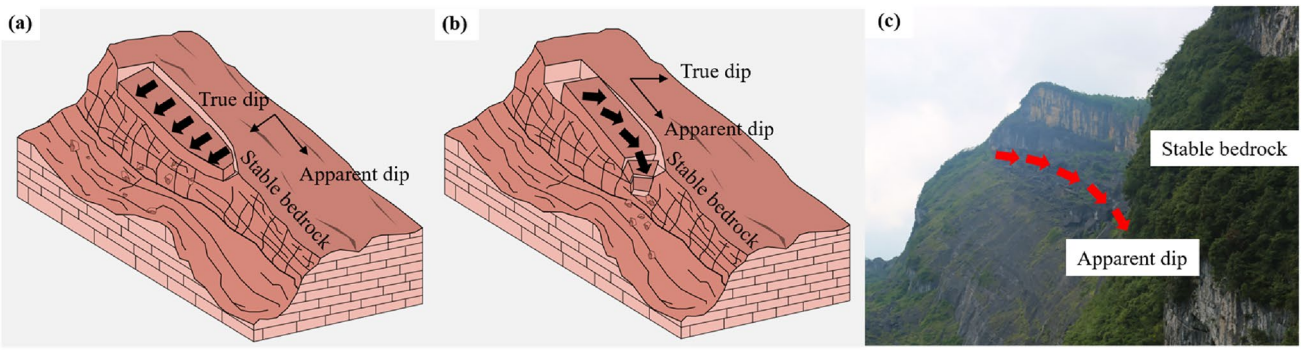

Fig. 13 Mining-induced landslides in oblique inclined bedding layered slope. **a** Schematic diagram of rock planar slide; **b** schematic diagram of rock apparent dip slide (Li et al. 2016b); **c** the Jiweishan landslide

prototype of the cantilever beam limit equilibrium model was first established by Aydan and Kawamoto (1992) on the basis of the superimposed cantilever beam model. After assuming the rupture surface is a straight line passing through the toe of the slope, the moment balance equation of each rock beam is established from top to the foot of slope, and the remaining sliding force is calculated iteratively to determine the stability of the slope. Then, scholars revised and improved the parameters of the cantilever beam limit equilibrium model (Adhikary et al. 1997; Adhikary and Dyskin 2007; Bowa and Xia 2018; Zheng et al. 2020). Tao et al. (2019) considered the blasting vibration load generated by mining based on previous models. Xie et al. (2019) applied the improved cantilever beam limit equilibrium model to analyze the stability of mining slopes and proposed stability criteria; the models and formulas are as follows.

Figure 14a is a simplified geomechanical model of steep slope induced by open-pit mining. In this model, the rupture surface no longer passes through the toe of the slope, but as a straight line through the vertex of the remaining ore layer. Comparison of the length of each rock beam above the rupture surface with the length of fracture induced by self-weight shows that when the former is longer than the latter, flexural topple (a few rock beams might shear and slide) would happen. The cantilever beam limit equilibrium model is shown in Fig. 14b.

When rock beam k is toppling, the toppling resistance P_k of the underlying rock beam acting on the rock beam k is:

$$P_k = \frac{\rho g l_k^2 b\cos\beta - b^2\left(\sigma + \rho g l_k \sin\beta\right)/3}{l_k + b\tan\varphi_j}, \tag{1}$$

where, $l_k = \frac{b\sin(\pi/2-\beta)+\sqrt{b^2\sin^2(\pi/2-\beta)+12b\cos(\pi/2-\beta)\sigma/\gamma}}{6\cos(\pi/2-\beta)}$; l_k is the fracture length of the rock beam induced by self-weight; ρ is the density of the rock beam; γ is the gravity of the rock beam; φ is the friction angle of the rock beam; φ_j is the bedding friction angle; c is the cohesion of the rock beam; b is thickness of the rock beam; $180° - \theta$ is the inclination normal angle of the rock beam; β is the inclination angle of the rock beam; σ is the tensile strength of the rock beam.

When rock beam k is sliding, the sliding resistance F_k of the underlying rock beam acting on the rock beam k is:

$$F_k = \frac{\rho g b\cos\theta\cos(\alpha-\theta)(\tan\varphi+\tan\theta)l_k - cbk}{\cos^2(\alpha-\theta)\left\{1+\tan\varphi_j\tan(\alpha-\theta)+\tan\varphi\left[\tan(\alpha-\theta)-\tan\varphi_j\right]\right\}}. \tag{2}$$

The failure modes and stability criteria are:

1. $T = \max\left(P_1, F_1\right) < 0$.

   The slope is unstable. If $P_i \geq F_i$, it will flexurally topple; if $P_i < F_i$ and $P_{i+1} > F_{i+1}$ $(1 \leq i < m)$, the failure mode will be flexural topple slide, that is, rock beams

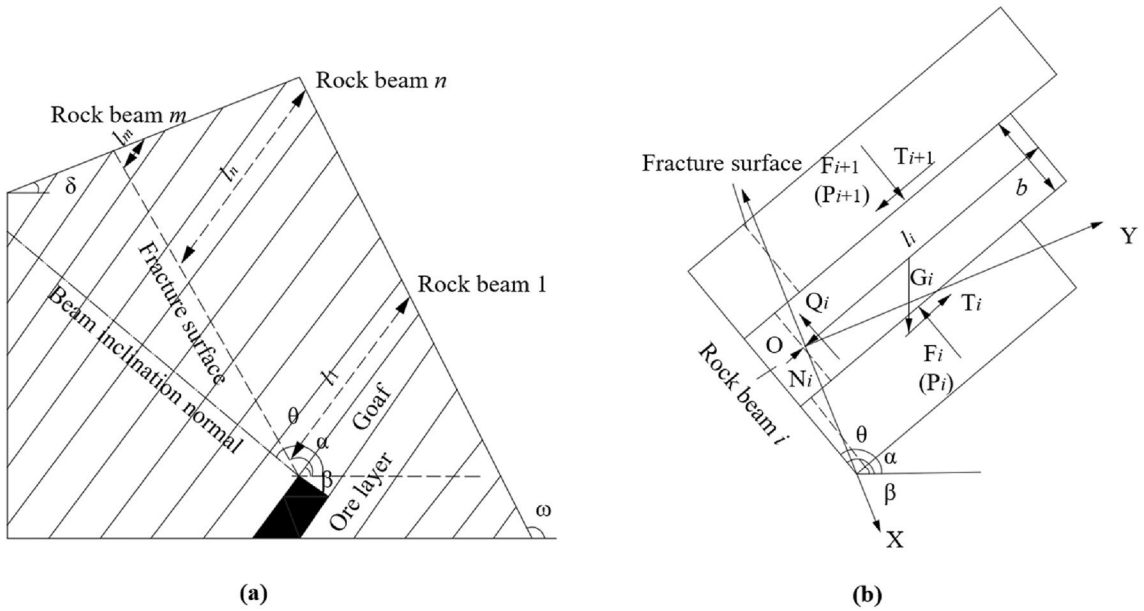

Fig. 14 Cantilever beam limit equilibrium model for mining-induced rock flexural topple. **a** Simplified geomechanically model; **b** cantilever beam limit equilibrium model (Xie et al. 2019)

below i will be sheared off and slide, and rock beams above i will flexurally topple.

2. $T = \max\left(P_1, F_1\right) = 0$.
   The slope is at limiting equilibrium.
3. $T = \max\left(P_1, F_1\right) > 0$.

The slope is stable.

Cantilever beam model for rock planar slide

For the failure mode of rock planar slide which slides along the bedding, Tang et al. (2015) proposed a progressive locking mechanical model and deduced the calculation formula for the stability of progressive failure slopes. Based on this, Tang et al. (2019) and Dai (2019) took the impact of mining bending and subsidence into account, and the geomechanical model and cantilever beam model are shown in Fig. 15a, b. This model considered the separation phenomenon caused by mining-induced uncoordinated deformation of hard rock and underlying weak structural layers. The weak structural layer is regarded as a viscoelastic foundation, and the hard rock is regarded as a cantilever beam. The separation length l reflects the range of mining disturbance. With the continuous excavation of underground mining, the separation length l gradually increases. When the tensile stress of hard rock reaches tensile strength, the fractured rock mass falls on the weak structural layer.

The subsidence of the rock slope and weak structural layer at the moment t at point x is:

$$W(x,t) = (1 - e^{-kt})e^{-\alpha x}\frac{P_z l}{4IE_p(w)\alpha^2}\left[l\sin(\alpha x) - \left(\frac{2}{\alpha} + l\right)\cos(\alpha x)\right], \tag{1}$$

where α is the rock mass characteristic coefficient ($\alpha = (\frac{E_r(w)}{4IE_p(w)m})^{1/4}$), P_z is the slope body load, $P_z = \gamma h\cos\theta$; $k = \frac{E_p(w)}{\eta_p(w)} = \frac{E_r(w)}{\eta_r(w)}$, $E_p(w)$ is the elastic modulus of the slope, $\eta_p(w)$ is the viscosity coefficient of the rock slope, $E_r(w)$ is the elastic modulus of the weak structural layer, $\eta_r(w)$ is the viscosity coefficient of the weak structural layer, m is the thickness of the weak structural layer, I is the cross-sectional moment of inertia of the slope with respect to the y-axis, γ is the volume weight of the slope, h is the slope thickness, θ is the slope angle, and l is the separation length.

The bending moment of the rock mass in the slope is:

$$M(x,t) = -\frac{P_z l}{2}(1 - \mathrm{e}^{-kt})\mathrm{e}^{-\alpha x}\left[\frac{(2+\alpha l)}{\alpha}\sin(\alpha x) + l\cos(\alpha x)\right]. \tag{2}$$

The stress in the slope is:

$$\sigma(x,t) = -\frac{P_z l z}{2I}(1 - e^{-kt})\mathrm{e}^{-\alpha x}\left[\frac{(2+\alpha l)}{\alpha}\sin(\alpha x) + l\cos(\alpha x)\right] + \gamma h\sin\theta. \tag{3}$$

The sliding resistance of the fractured rock mass (per unit width) is:

$$F_{K1}(x) = \int_{-l}^{x_{\sigma\max}} (\gamma h\cos\theta_2\mu\tan\varphi_0 + \mu C_0)\mathrm{d}x, \tag{4}$$

where, μ is the weakening factor, $\mu = \frac{\tan(\varphi)}{\tan(\varphi_0)} = \frac{C}{C_0}$, C_0 is cohesive force of weak structural layer before weakening, C is cohesive force of weakened weak structural layer, φ_0 is

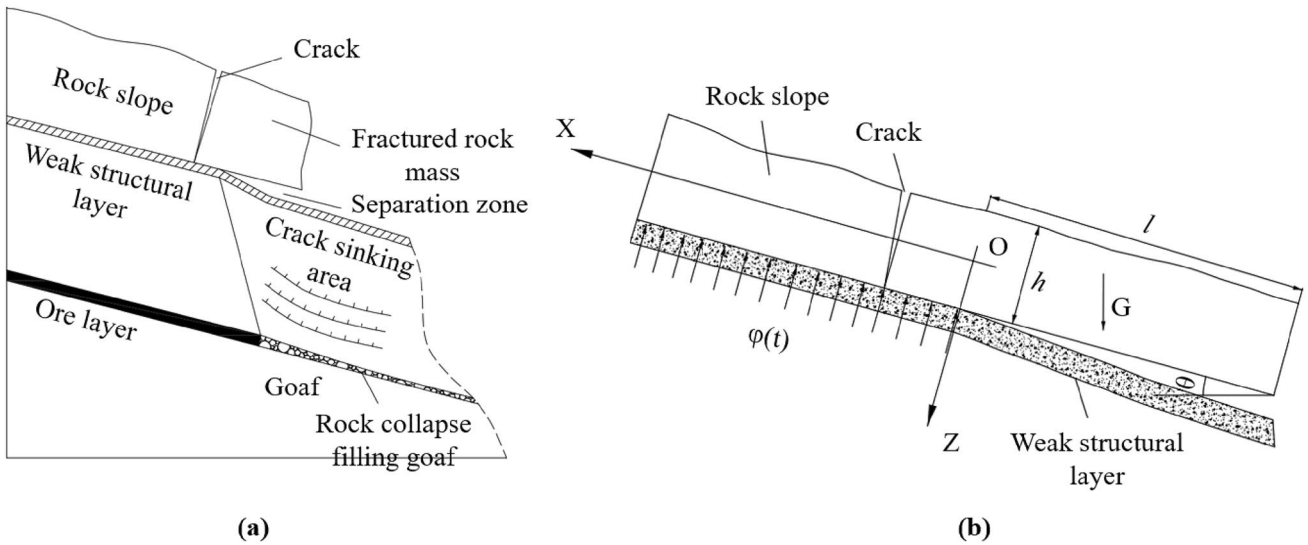

Fig. 15 Cantilever beam model for mining-induced rock planar slide. **a** Geomechanically model; **b** cantilever beam model (Tang et al. 2019)

friction angle of weak structure layer before weakening, φ is friction angle of weakened weak structural layer; θ_2 is slope inclination angle of fractured rock mass.

The sliding force of the fractured rock mass (per unit width) is:

$$F_{X1}(x) = \int_{-l}^{x_{\sigma\max}} (\gamma h \sin\theta_2)\mathrm{d}x. \tag{5}$$

Therefore, the stability factor of the fractured rock mass is:

$$F_{\mathrm{r}} = \frac{\mu(\gamma h \cos\theta_2 \tan\varphi_0 + C_0)}{\gamma h \sin\theta_2}. \tag{6}$$

The failure modes and stability criteria are:

1. If $F_{\mathrm{r}} > 1$, the sliding resistance is greater than the sliding force, the slope is stable but forms a dangerous rock mass.
2. If $F_{\mathrm{r}} = 1$, the sliding resistance is equal to the sliding force, and the slope is at limiting equilibrium.
3. If $F_{\mathrm{r}} < 1$, the sliding force is greater than the sliding resistance, forming a rock planar slide.

Discussion

In this paper, the environmental characteristics and triggering factors of landslides in karst mountains areas of southwestern China were systematically analyzed by investigating large-scale landslides in the mining areas of Southwest China, and the triggering mechanism of each natural condition and human activity were clarified. The mechanism of each natural condition and human activity were clarified. Based on the Varnes (1978) landslide classification system adopted by WP/WLI and according to the layered slope classification by Liu et al. (1993), a relatively unified classification system for mining landslide in the southwestern karst mountainous areas of southwestern China is established (Table 3), and the basic failure modes and influence of mining activities of five common layered slopes are described in detail.

However, since mining landslides are caused by different geological environments and human engineering activities, the slight differences in the geological environment and mining activities would lead to different failure modes. The classification system of mining landslide summarized in this paper may not completely cover all the failure modes in complex conditions (e.g., some mining landslide modes might be the combined modes of these basic modes). Thus, a priority for further research should be to discuss the combined modes of mining landslides. In addition, although scholars have noticed that mining would induce landslides and have analyzed its causes, the current researches on the mechanical model of mining landslides is relatively hysteretic. The mature mechanical models mainly include the cantilever beam limit equilibrium model for the failure mode of mining flexural toppling and the cantilever beam model for mining planar slide. However, these two models are not suitable for all mining landslide failure modes. Therefore, the theoretical study of slope stability and its unstable mechanism induced by mining still needs to be further researched. Besides, the distribution of karst fissures, conduits and caves in soluble rocks has the characteristics of randomness and complexity, resulting in heterogeneity of the rock strata. Presently, scholars have done a lot of researches in identifying karst characteristics and groundwater system model for a certain area or a specific slope, but how to reflect these heterogeneous karst characteristics in theoretical models, even model tests and numerical simulations and how to couple with mining activities still need to be further explored.

Conclusions

Mining landslides in the karst mountainous area of southwestern China are disasters caused by the geological environment (topography, lithology, geological structure, karst hydrogeology and rainfall) and human engineering activities (mining activities), while geological environment factors

Table 3 Unified failure mode classification system for mining landslides

Slope types	Failure modes		
Subhorizontal bedding layered slope	Rock rotational slide	Rock block topple	Rock collapse
Bedding layered slope	Rock planar slide		
Anti-dip layered slope	Rock rotational slide (gentle slope)		
	Rock flexural topple (steep slope)		
Lateral layered slope	Rock flexural topple (steep slope)		
Oblique inclined bedding layered slope	Rock planar slide (inclined outside slope)		Rock apparent dip slide (inclined inside slope)

('boat-shaped' topography, structure of soft–hard interbedding or hard–soft–hard interlayer, dominant discontinuities, hydrogeology with strong dissolution, abundant and intense rainfall) are the primary inducements, and frequent long-term mining activities directly lead to or greatly accelerate the occurrence of landslides.

Due to the complicated environmental conditions, the failure mechanisms of mining landslides in the karst mountainous areas of Southwest China are also complex. Thus, a unified mining landslide classification system is the basic tool to prevent and control these disasters. In this paper, a unified classification system of mining landslide failure modes is established, where the terms in different landslide classification due to different evaluation indicators and analysis methods are unified, and the affected mechanism of mining on each failure mode in the classification system is clarified. In this classification system, there are five different slopes types: subhorizontal bedding layered slopes, bedding layered slopes, anti-dip layered slopes, lateral layered slopes, and oblique inclined bedding layered slopes. The failure modes of subhorizontal bedding layered slope are generally rock rotational slide, rock block topple and rock collapse. The failure of rock planar slide occurs mainly in bedding layered slopes. The failure mode for anti-dip layered gentle slope is rock rotational slide, while for anti-dip layered steep slope it is rock flexural topple. The failure mode of lateral layered steep slope is more likely to be the mode of anti-dip layered steep slope. The oblique inclined bedding layered slope whose inclination outside the slope would occur on the planar slide, and the special inclination outside the slopes ones might form an apparent dip slide. Accordingly, mechanical models and stability criteria for mining-induced flexural topple and planar slide are summarized to facilitate future research.

Acknowledgements This research was financially supported by the National Natural Science Foundation of China (no. 52074042) and the National Key R&D Program of China (no. 2018YFC1504802). The authors are sincerely thankful to Profs. Bin Li, Zhongping Yang, FangPeng Cui and Dr. Fei Xiong for their great support to this study.

Author contributions All authors contributed to the study conception and design. ZZ had the initial idea for the manuscript, YX performed the literature search and data analysis, ZZ and YX drafted the manuscript and revised most of the manuscript according to reviewers' comments, NW put forward detailed modification ideas, crucial for the revised manuscript and drew some modified figures, and XL and GG commented on previous versions of the manuscript and provided some modification suggestions.

Funding This work was supported by the National Natural Science Foundation of China (no. 52074042) and National Key R&D Program of China (no. 2018YFC1504802).

Availability of data and material All authors consent to publish all data and materials and comply with field standards.

Code availability Not applicable (this manuscript has no software application or custom code).

Declarations

Conflicts of interest The authors have no relevant financial or non-financial interests to disclose.

Ethics approval Not applicable.

Consent to participate Not applicable.

Consent for publication Not applicable.

References

Adhikary DP, Dyskin AV (2007) Modelling of progressive and instantaneous failures of foliated rock slopes. Rock Mech Rock Eng 40(4):349–362. https://doi.org/10.1007/s00603-006-0085-8

Adhikary DP, Dyskin AV, Jewell RJ, Stewart DP (1997) A study of the mechanism of flexural toppling failure of rock slopes. Rock Mech Rock Eng 30(2):75–93. https://doi.org/10.1007/BF01020126

Ali S, Kamran E, Bibhu M (2018) Degradation of a discrete infilled joint shear strength subjected to repeated blast-induced vibrations. Int J Min Sci Technol 28(4):561–571. https://doi.org/10.1016/j.ijmst.2018.04.015

Arca D, Kutoglu HS, Becek K (2018) Landslide susceptibility mapping in an area of underground mining using the multicriteria decision analysis method. Environ Monit Assess. https://doi.org/10.1007/s10661-018-7085-5

Aydan Ö, Kawamoto T (1992) The stability of slopes and underground openings against flexural toppling and their stabilisation. Rock Mech Rock Eng 25(3):143–165. https://doi.org/10.1007/BF01019709

Ban YX, Fu X, Xie Q, Cui JF, Xu H (2021) A simplified calculation method for ultimate mining dimension in thin coal seam. Geotech Geol Eng (prepublish). https://doi.org/10.1007/S10706-021-01717-Y

Benko B, Stead D (1998) The Frank slide: a reexamination of the failure mechanism. Can Geotech J 35(2):299–311. https://doi.org/10.1139/t98-005

Bentley SP, Siddle HJ (1996) Landslide research in the South Wales coalfield. Eng Geol 43(1):65–80. https://doi.org/10.1016/0013-7952(95)00084-4

Bowa VM, Xia YY (2018) Stability analyses of jointed rock slopes with counter-tilted failure surface subjected to block toppling failure mechanisms. Arab J Sci Eng 43(10):5315–5331. https://doi.org/10.1007/s13369-018-3168-4

Chen HR, Qin SQ, Xue L, Yang BC, Zhang K (2018) A physical model predicting instability of rock slopes with locked segments along a potential slip surface. Eng Geol 242:34–43. https://doi.org/10.1016/j.enggeo.2018.05.012

Chen LQ, Zhao CY, Li B, He K, Ren CF, Liu XJ, Liu DL (2021) Deformation monitoring and failure mode research of mining-induced Jianshanying landslide in karst mountain area, China with ALOS/PALSAR-2 images. Landslides 18:2739–2750. https://doi.org/10.1007/s10346-021-01678-6

Cipriano DM, Giuliana M, Marco V (2014) Deep-seated gravitational slope deformations in western Sicily: controlling factors, triggering mechanisms, and morphoevolutionary models. Geomorphology 208:173–189. https://doi.org/10.1016/j.geomorph.2013.11.023

Cui FP, Li B, Xiong C, Yang ZP, Peng JQ, Li JS, Li HW (2022) Dynamic triggering mechanism of the Pusa mining-induced landslide in Nayong County, Guizhou Province, China. Geomat Nat Haz Risk 13(1):123–147. https://doi.org/10.1080/19475705.2021.2017020

Dahal RK, Hasegawa S (2008) Representative rainfall thresholds for landslides in the Nepal Himalaya. Geomorphology 100(3–4):429–433. https://doi.org/10.1016/j.geomorph.2008.01.014

Dai ZY (2019) Study on deformation and failure mechanism and similar simulation test of consequent bedding rock slope after underground mining. Dissertation, Chongqing University, China **(in Chinese)**

Di Maggio C, Madonia G, Vattano M (2014) Deep-seated gravitational slope deformations in western Sicily: controlling factors, triggering mechanisms, and morphoevolutionary models. Geomorphology 208:173–189. https://doi.org/10.1016/j.geomorPh.2013.11.023

de Freitas MH, Watters RJ (1973) Some field examples of toppling failure. Geotechnique 23(4):495–513. https://doi.org/10.1680/geot.1973.23.4.495

Deniz A, Hakan SK, Kazimierz B (2018) Landslide susceptibility mapping in an area of underground mining using the multicriteria decision analysis method. Environ Monit Assess. https://doi.org/10.1007/s10661-018-7085-5

Detwiler RL, Rajaram H (2007) Predicting dissolution patterns in variable aperture cracks: evaluation of an enhanced depth-averaged computational model. Water Resour Res. https://doi.org/10.1029/2006WR005147

Do TN, Wu JH (2020) Simulating a mining-triggered rock avalanche using DDA: a case study in Nattai North, Australia. Eng Geol. https://doi.org/10.1016/j.enggeo.2019.105386

Erginal AE, Türkes M, Ertek TA, Baba A, Bayrakdar C (2008) Geomorphological investigation of the excavation-induced Dündar landslide, Bursa—Turkey. Geogr Ann A 90(2):109–123. https://doi.org/10.1111/j.1468-0459.2008.00159.x

Fan XM, Xu Q, Scaringi G, Zheng G, Huang RQ, Dai LX, Ju YZ (2019) The "long" runout rock avalanche in Pusa, China, on August 28, 2017: a preliminary report. Landslides 16(1):139–154. https://doi.org/10.1007/s10346-018-1084-z

Feng L (2013) Failure models of nearly horizontal rock slopes with the upper hard and lower soft. Dissertation, Chengdu University of Technology, China **(in Chinese)**

Feng Z, Li B, Yin YP, He K (2014) Rockslides on limestone cliffs with subhorizontal bedding in the southwestern calcareous area of China. Nat Hazard Earth Sys 14(9):2627–2635. https://doi.org/10.5194/nhess-14-2627-2014

Feng Z, Li B, Cai QP, Cao JW (2016) Initiation mechanism of the Jiweishan landslide in Chongqing, Southwestern China. Environ Eng Geosci. https://doi.org/10.2113/gseegeosci.22.4.341

Ge YF, Tang HM, Ez Eldin MAM, Chen HZ, Zhong P, Zhang L, Fang K (2019) Deposit characteristics of the Jiweishan rapid long-runout landslide based on field investigation and numerical modeling. B Eng Geol Environ 78(6):4383–4396. https://doi.org/10.1007/s10064-018-1422-3

Goeppert N, Goldscheider N, Scholz H (2011) Karst geomorphology of carbonatic conglomerates in the Folded Molasse zone of the Northern Alps (Austria/Germany). Geomorphology 130(3–4):289–298. https://doi.org/10.1016/j.geomorph.2011.04.011

Goodman RE, Bray JW (1976) Toppling of rock slopes. In: Proceedings of ASCE specialty conference on rock engineering for foundations and slopes, pp 201–234

Gu DM, Huang D, Yang WD, Zhu JL, Fu GY (2017) Understanding the triggering mechanism and possible kinematic evolution of a reactivated landslide in the Three Gorges Reservoir. Landslides 14(6):2073–2087. https://doi.org/10.1007/s10346-017-0845-4

He K, Chen CL (2014) Stability analysis of Puzi landslide in Chongqing. Appl Mech Mater 580–583:923–926. https://doi.org/10.4028/www.scientific.net/AMM.580-583.923

He KQ, Yu GM, Li XR (2009) The regional distribution regularity of landslides and their effects on the environments in the Three Gorges Reservoir Region, China. Environ Geol. https://doi.org/10.1007/s00254-008-1482-y

He K, Chen CL, Li B (2019a) Case study of a rockfall in Chongqing, China: movement characteristics of the initial failure process of a tower-shaped rock mass. B Eng Geol Environ 78(5):3295–3303. https://doi.org/10.1007/s10064-018-1364-9

He K, Yin YP, Li B, Chen CL (2019b) The mechanism of the bottom-crashing rockfall of a massive layered carbonate rock mass at Zengziyan, Chongqing, China. J Earth Syst Sci. https://doi.org/10.1007/s12040-019-1141-6

Hoek E, Bray J (1981) Rock slope engineering. The Institute of Mining and Metallurgy, London

Hu QJ, Shi RD, Zheng LN, Cai QJ, Du LQ, He LP (2018) Progressive failure mechanism of a large bedding slope with a strain-softening interface. B Eng Geol Environ 77(1):69–85. https://doi.org/10.1007/s10064-016-0996-x

Hu J, Liu HL, Li LP, Zhou S, Zhang Q, Sun SQ (2019) Stability analysis of dangerous rockmass considering rainfall and seismic activity with a case study in China's Three Gorges area. Pol J Environ Stud 28(2):631–645. https://doi.org/10.15244/pjoes/78925

Huang RQ (2015) Understanding the mechanism of large-scale landslides. In: Lollino G, Giordan D, Crosta GB, Corominas J, Azzam R, Wasowski J, Sciarra N (eds) Engineering geology for society and territory—volume 2: landslide processes. Springer, Cham. https://doi.org/10.1007/978-3-319-09057-3_2

Huang D, Yang WD, Chen ZQ (2018) Analysis on collapse mechanism of Wangxia dangerous rock considering weathering effect of weak foundation. Yangtze River 49(06):64–69+78. https://doi.org/10.1623/j.cnki.1001-4179.2018.06.011 ((**in Chinese**))

Hungr O, Leroueil S, Picarelli L (2014) The Varnes classification of landslide types, an update. Landslides 11(2):167–194. https://doi.org/10.1007/s10346-013-0436-y

International Geotechnical Society's UNESCO Working Party on World Landslide Inventory (WP/WLI) (1990) A suggested method for reporting a landslide. Bull Inter Assoc Eng Geol 41:5–12. https://doi.org/10.1007/bf02590201

Jian L, Gao JG, Dao Y (2014) The elemental association characteristics of Pb-Zn deposits in the Sichuan-Yunnan-Guizhou border area in Southwest China. Adv Mater Res 868:117–120. https://doi.org/10.4028/www.scientific.net/AMR.868.117

Jiang XZ, Lei MT, Gao YL (2017) Formation mechanism of large sinkhole collapses in Laibin, Guangxi, China. Environ Earth Sci. https://doi.org/10.1007/s12665-017-7128-1

Kulatilake Pinnaduwa HSW, Ge YF (2014) Investigation of stability of the critical rock blocks that initiated the Jiweishan landslide in China. Geotech Geol Eng 32(5):1291–1315. https://doi.org/10.1007/s10706-014-9806-z

Li AH, Wang SJ (1994) Progressive failure model for slope with plane sliding surface and its application. J Eng Geol 2(1):1–8

Li WX, Wen L, Liu XM, Hou XB, Liu L (2009) Regional horizontal displacements and its effect on shaft in mining areas. Chin J Rock Mech Eng 8(S2):3926–4190 ((**in Chinese**))

Li B, Feng Z, Wang GZ, Wang WP (2016a) Processes and behaviors of block topple avalanches resulting from carbonate slope failures due to underground mining. Environ Earth Sci. https://doi.org/10.1007/s12665-016-5529-1

Li B, Feng Z, Zhang Q, Zhao CY, Yan JK et al (2016b) Study on disaster mode and early identification of catastrophic landslide disaster in karst mountainous area. Science Press, Beijing ((**in Chinese**))

Li ZQ, Xue YG, Li SC, Zhang LW, Wang D, Li B, Zhang W, Ning K, Zhu JY (2017) Deformation features and failure mechanism of steep rock slope under the mining activities and rainfall. J Mt Sci-Engl 14(1):31–45. https://doi.org/10.1007/s11629-015-3781-6

Li H, Zhong ZL, Liu XR, Sheng Y, Yang DM (2018) Micro-damage evolution and macro-mechanical property degradation of limestone due to chemical effects. Int J Rock Mech Min 110:257–265. https://doi.org/10.1016/j.ijrmms.2018.07.011

Li ZW, Xu XL, Zhu JX, Xu CH, Wang KL (2019) Effects of lithology and geomorphology on sediment yield in karst mountainous catchments. Geomorphology 343:119–128. https://doi.org/10.1016/j.geomorph.2019.07.001

Li H, Zhong ZL, Eshiet KII et al (2020a) Experimental investigation of the permeability and mechanical behaviours of chemically corroded limestone under different unloading conditions. Rock Mech Rock Eng 53(4):1587–1603. https://doi.org/10.1007/s00603-019-01961-y

Li J, Zhu HL, Li B, He K, Gao Y (2020b) Key problems of mining induced collapse and slide disaster in mountainous area of coal measure strata in Southwest China. Carsol Sin 39(4):453–466 (**(in Chinese)**)

Li SC, Wang XT, Xu ZH, Mao DQ, Pan DD (2021) Numerical investigation of hydraulic tomography for mapping karst conduits and its connectivity. Eng Geol. https://doi.org/10.1016/j.enggeo.2020.105967

Li T, Chen M, Wei D, Lu WB, Yan P (2022) Disturbance effect of blasting stress wave on crack of rock mass in water-coupled blasting. KSCE J Civ Eng. https://doi.org/10.1007/s12205-022-1837-z

Lin F, Wu LZ, Huang RQ, Zhang H (2018) Formation and characteristics of the Xiaoba landslide in Fuquan, Guizhou, China. Landslides 15(4):669–681. https://doi.org/10.1007/s10346-017-0897-5

Liu HC, Chen MD, Li KW, Hu XW, Liu WZ, Liu JD (1993) Study on environmental geological evaluation of reservoir area. Chengdu, China **(in Chinese)**

Luo K, Zhou JX, Huang ZL, Wang XC, Wilde SA, Zhou W, Tian LY (2019) New insights into the origin of early Cambrian carbonate-hosted Pb–Zn deposits in South China: a case study of the Maliping Pb–Zn deposit. Gondwana Res 70:88–103. https://doi.org/10.1016/j.gr.2018.12.015

Lv XF, Zhou HY, Wang ZW, Cai Y (2018) Movement and failure law of slope and overlying strata during underground mining. J Geophys Eng 15(4):1638–1650. https://doi.org/10.1088/1742-2140/aab8b2

Marian M, Işık Y, Martin B, Karel K (2012a) Influence of underground mining activities on the slope deformation genesis: Doubrava Vrchovec, Doubrava Ujala and Staric case studies from Czech Republic. Eng Geol 147:37–51. https://doi.org/10.1016/j.enggeo.2012.07.014

Marian M, Işık Y, Martin B, Karel K (2012b) Deformation of slopes as a cause of underground mining activities: three case studies from Ostrava-Karviná coal field (Czech Republic). Environ Monit Assess 184(11):6709–6733. https://doi.org/10.1007/s10661-011-2453-4

Martha TR, Roy P, Govindharaj KB, Kumar KV, Diwakar PG, Dadhwal VK (2015) Landslides triggered by the June 2013 extreme rainfall event in parts of Uttarakhand state, India. Landslides 12(1):135–146. https://doi.org/10.1007/s10346-014-0540-7

Moosavi E, Shirinabadi R, Gholinejad M (2016) Prediction of seepage water pressure for slope stability at the Gol-E-Gohar open pit mine. J Min Sci 52(6):1069–1079. https://doi.org/10.1134/S1062739116061601

Nunoo S (2018) Lessons learnt from open pit wall instabilities: case studies of BC open pit hard rock mines. J Min Sci 54(5):804–812. https://doi.org/10.1134/S1062739118054915

Poisel R, Bednarik M, Holzer R, Liščák P (2005) Geomechanics of hazardous landslides. J Mt Sci-Engl. https://doi.org/10.1007/BF02973194

Poisel R, Angerer H, Pöllinger M, Kalcher T, Kittl H (2009) Mechanics and velocity of the Lärchberg-Galgenwald landslide (Austria). Eng Geol 109(1):57–66. https://doi.org/10.1016/j.enggeo.2009.01.002

Rohn J, Resch M, Schneider H, Fernandez-Steeger TM, Czurda K (2004) Large-scale lateral spreading and related mass movements in the Northern Calcareous Alps. B Eng Geol Environ. https://doi.org/10.1007/s10064-003-0201-x

Salmi EF, Nazem M, Karakus M (2017) Numerical analysis of a large landslide induced by coal mining subsidence. Eng Geol 217:141–152. https://doi.org/10.1016/j.enggeo.2016.12.021

Stephen PB, Howard JS (1996) Landslide research in the South Wales coalfield. Eng Geol 43(1):65–80. https://doi.org/10.1016/0013-7952(95)00084-4

Sun SQ, Li LP, Li SC, Zhang QQ, Hu C (2017) Rockfall hazard assessment on Wangxia Rock Mass in Wushan (Chongqing, China). Geotech Geol Eng 35(4):1895–1905. https://doi.org/10.1007/s10706-017-0203-2

Tang FQ (2009) Research on mechanism of mountain landslide due to underground mining. J Coal Sci Eng (china) 15(4):351–354. https://doi.org/10.1007/s12404-009-0403-3

Tang HM, Zou ZX, Xiong CR, Wu YP, Hu XL, Wang LQ, Lu S, Criss RE, Li CD (2015) An evolution model of large consequent bedding rockslides, with particular reference to the Jiweishan rockslide in Southwest China. Eng Geol 186:17–27. https://doi.org/10.1016/j.enggeo.2014.08.021

Tang JX, Dai ZY, Wang YL, Zhang L (2019) Fracture failure of consequent bedding rock slopes after underground mining in mountainous area. Rock Mech Rock Eng 52(8):2853–2870. https://doi.org/10.1007/s00603-019-01876-8

Tao ZG, Geng Q, Zhu C, He MC, Cai H, Pang SH, Meng XZ (2019) The mechanical mechanisms of large-scale toppling failure for counter-inclined rock slopes. J Geophys Eng 16(3):541–558. https://doi.org/10.1093/jge/gxz020

Vanneschi C, Eyre M, Venn A, Coggan JS (2019) Investigation and modeling of direct toppling using a three-dimensional distinct element approach with incorporation of point cloud geometry. Landslides 16(8):1453–1465. https://doi.org/10.1007/s10346-019-01192-w

Varnes DJ (1978) Slope movement types and processes. In: Schuster RL, Krizek RJ (eds) Landslides, analysis and control, special report 176: transportation research board. National Academy of Sciences, Washington, DC

Wang FW, Li TL (2009) Landslide disaster mitigation in Three Gorges Reservoir, China. Springer, Berlin

Wang ZQ, Yan EC, Yin XM, Zhang QM, Tang RX (2014) Study on collapse mechanism of anti inclined rock slope: a case study of Honglianchi Iron Mine slope in Hefeng, Hubei Province. J Cent South Univ (sci Tech) 45(07):2295–2302 (**(in Chinese)**)

Wang LY, Chen WZ, Tan XY, Tan XJ, Yuan JQ, Liu Q (2019) Evaluation of mountain slope stability considering the impact of geological interfaces using discrete fractures model. J Mt Sci-Engl 16(09):2184–2202. https://doi.org/10.1007/s11629-019-5527-3

Wang J, Wang C, Xie C, Zhang H, Tang YX, Zhang ZJ, Shen CY (2020) Monitoring of large-scale landslides in Zongling, Guizhou, China, with improved distributed scatterer interferometric SAR time series methods. Landslides 17(8):1777–1795. https://doi.org/10.1007/s10346-020-01407-5

Wu Y, He SM, Li XP (2010) Mechanism of action of cracks water on rock landslide in rainfall. J Cent South Univ T 17(6):1383–1388. https://doi.org/10.1007/s11771-010-0646-6

Xia KZ, Chen CX, Liu XM, Fu H, Pan YC, Deng YY (2016) Mining-induced ground movement in tectonic stress metal mines: a case study. B Eng Geol Environ 75(3):1089–1115. https://doi.org/10.1007/s10064-016-0886-2

Xie LF, Yan EC, Ren XB, Lu GD (2015) Sensitivity analysis of bending and toppling deformation for anti-slope based on the grey relation method. Geotech Geol Eng 33(1):35–41. https://doi.org/10.1007/s10706-014-9817-9

Xie HB, Ji ZW, Xu ZF, Chen HQ (2019) Study on the stability criteria of anti-dipped mountain above goaf. J HeNan Polytech Univ (nat Sci) 38(03):32–40 ((**in Chinese**))

Xing AG, Xu Q, Zhu YQ, Zhu JL, Jiang Y (2016) The August 27, 2014, rock avalanche and related impulse water waves in Fuquan, Guizhou, China. Landslides 13(2):411–422. https://doi.org/10.1007/s10346-016-0679-5

Xiong F, Liu XR, Ran Q, Li B, Zhong ZL, Yang ZP, Zhou XH (2021) Study on instability failure mechanism of karst mountain with deep and large fissures under the mining-fissure water coupling. J China Coal Soc 46(11):3445–3458. https://doi.org/10.1322/j.cnki.jccs.2020.1690

Xu Q, Fan XM, Huang RQ, Yin YP, Hou SS, Dong XJ, Tang MG (2010) A catastrophic rockslide-debris flow in Wulong, Chongqing, China in 2009: background, characterization, and causes. Landslides 7(1):75–87. https://doi.org/10.1007/s10346-009-0179-y

Xu T, Xu Q, Deng ML, Ma TH, Yang TH, Tang CA (2014) A numerical analysis of rock creep-induced slide: a case study from Jiweishan Mountain, China. Environ Earth Sci 72(6):2111–2128. https://doi.org/10.1007/s12665-014-3119-7

Xu Q, Liu H, Ran J, Li W, Sun X (2016) Field monitoring of groundwater responses to heavy rainfalls and the early warning of the Kualiangzi landslide in Sichuan Basin, southwestern China. Landslides 13(6):1555–1570. https://doi.org/10.1007/s10346-016-0717-3

Yang YC, Xing HG, Yang XG, Chen ML, Zhou JW (2018) Experimental study on the dynamic response and stability of bedding rock slopes with weak interlayers under heavy rainfall. Environ Earth Sci. https://doi.org/10.1007/s12665-018-7624-y

Yin YP, Sun P, Zhang M, Li B (2011) Mechanism on apparent dip sliding of oblique inclined bedding rockslide at Jiweishan, Chongqing, China. Landslides 8(1):49–65. https://doi.org/10.1007/s10346-010-0237-5

Yu XY, Mao XW (2020) A preliminary discrimination model of a deep mining landslide and its application in the Guanwen coal mine. B Eng Geol Environ. https://doi.org/10.1007/s10064-019-01565-4

Yu D, Huang XH, Li ZY (2020a) Variation patterns of landslide basal friction revealed from long-period seismic waveform inversion. Nat Hazards 100(1):313–327. https://doi.org/10.1007/s11069-019-03813-y

Yu JL, Zhao JJ, Yan HY, Lai QY, Huang RQ, Liu XW, Li YC (2020b) Deformation and failure of a high-steep slope induced by multi-layer coal mining. J Mt Sci-Engl 17(12):2942–2960. https://doi.org/10.1007/S11629-019-5941-6

Zhang Q, López DL (2019) Use of time series analysis to evaluate the impacts of underground mining on the hydraulic properties of groundwater of dysart woods, Ohio. Mine Water Environ 38(3):566–580. https://doi.org/10.1007/s10230-019-00619-z

Zhang YN, Tang JX, Li GD, Teng JY (2016) Influence of depth-thickness ratio of mining on the stability of a bedding slope with its sliding surface in concave deformation. Int J Min Sci Technol 26(6):1117–1123. https://doi.org/10.1016/j.ijmst.2016.09.022

Zhang M, McSaveney M, Shao H, Zhang CY (2018) The 2009 Jiweishan rock avalanche, Wulong, China: precursor conditions and factors leading to failure. Eng Geol 233:225–230. https://doi.org/10.1016/j.enggeo.2017.12.010

Zhao JJ, Xiao JG, Lee ML, Ma YT (2016) Discrete element modeling of a mining-induced rock slide. Springerplus. https://doi.org/10.1186/s40064-016-3305-z

Zheng D, Frost JD, Huang RQ, Liu FZ (2015) Failure process and modes of rockfall induced by underground mining: a case study of Kaiyang Phosphorite Mine rockfalls. Eng Geol 197:145–157. https://doi.org/10.1016/j.enggeo.2015.08.011

Zheng Y, Chen CX, Meng F, Liu TT, Xia KZ (2020) Assessing the stability of rock slopes with respect to flexural toppling failure using a limit equilibrium model and genetic algorithm. Comput Geotech. https://doi.org/10.1016/j.compgeo.2020.103619

Zhu YQ, Xu SM, Zhuang Y, Dai XJ, Lv G, Xing AG (2019) Characteristics and runout behaviour of the disastrous 28 August 2017 rock avalanche in Nayong, Guizhou, China. Eng Geol. https://doi.org/10.1016/j.enggeo.2019.105154

Zuan P, Huang Y (2018) Prediction of sliding slope displacement based on intelligent algorithm. Wirel Pers Commun 102(4):3141–3157. https://doi.org/10.1007/s11277-018-5333-1